Chemical Engineering and Processing 97 (2015) 195–212

Contents lists available at ScienceDirect

Chemical Engineering and Processing: Process Intensification

journal homepage: www.elsevier.com/locate/cep

Periodic steady-state flow crystallization of a pharmaceutical drug using MSMPR operation

K.A. Powell [a,*], A.N. Saleemi [a], C.D. Rielly [a], Z.K. Nagy [a,b]

[a] EPSRC Centre in Continuous Manufacturing and Crystallisation at the Department of Chemical Engineering, Loughborough University, Loughborough, Leicestershire LE11 3TU, UK
[b] School of Chemical Engineering, Purdue University, West Lafayette, IN 47907, USA

ARTICLE INFO

Article history:
Received 10 April 2014
Received in revised form 15 December 2014
Accepted 7 January 2015
Available online 27 March 2015

Keywords:
Integrated PAT
PMSMPR
CryPRINS
Periodic steady-state
Flow crystallization
State of controlled operation

ABSTRACT

In this paper, a novel concept of periodic mixed suspension mixed product removal (PMSMPR) crystallization process is demonstrated. An integrated array of process analytical technologies (PATs), based on attenuated total reflectance ultra violet/visible spectroscopy, focused beam reflectance measurement, particle vision microscopy and Raman spectroscopy, and in-house developed crystallization process informatics system software (CryPRINS) were used to monitor the periodic steady-state flow crystallization of paracetamol. Periodic steady-state is a new concept defined as a state of a system that maintains itself despite transitory effects caused by periodic, but controlled disruptions (state of controlled operation). This work also illustrates the concept of "state of controlled operation" instead of "steady-state operation" as a state that can characterize continuous (periodic) operation. The PMSMPR was configured as either a single- or two-stage unit and operated for up to 11 residence times without blockage or encrustation problems. The number of PMSMPR stages, seed characteristics (size, shape and distribution), and use of recycle stream were the main variables that influenced the periodic operation, significantly affecting the extent of secondary nucleation and growth. The results further illustrate the use of PAT and information system tools together to determine when the periodic operation reaches a state of controlled operation (periodic steady-state). These tools provided a better understanding of the variables and operating procedures influencing the periodic operation.

1. Introduction

Process analytical technologies (PAT) and information systems can be used to design, analyze, and control pharmaceutical processes [1]. PAT such as attenuated total reflectance ultra violet/visible spectroscopy (ATR-UV/vis), attenuated total reflectance Fourier transform infra-red spectroscopy ATR-FTIR, near infrared spectroscopy (NIR), Raman, particle vision measurement (PVM) and focused beam reflectance measurement (FBRM) are widely used to monitor batch crystallizers [2–6]. However, few have combined integrated PAT array and information system tools to monitor continuous crystallizers, despite the potential to significantly improve pharmaceutical product quality, reduce waste and promote "greener", safer and more efficient manufacturing. Woo et al. [2] used an adaptive supersaturation control strategy based on FBRM counts/s and ATR-FTIR concentration measurements to detect the onset of nucleation and adapt the operating curve accordingly for the cooling and anti-solvent crystallization of paracetamol (PCM). Barrett et al. [3] used a so-called "calibration-free" approach based on ATR-FTIR, applying single peak tracking to monitor changes in supersaturation during the cooling crystallization of benzoic acid and an unnamed active pharmaceutical ingredient (API). Gherras et al. [4] demonstrated the application of an acoustic emission (AE) technique to monitor both solution and solid phase during the cooling crystallization of ammonium oxalate monohydrate. Hu et al. [5] used Raman spectroscopy to monitor quantitatively, the cooling crystallization of the enantiotropic polymorphic system flufenamic acid. Saleemi et al. [6] in their study to enhance the crystalline properties of the AstraZeneca API AZD7009 used ATR-UV/vis to monitor solution concentration and FBRM to apply automated direct nucleation control (ADNC) to prevent agglomeration and solvent inclusion. All of the studies mentioned above demonstrate the tremendous capabilities of PAT in process monitoring and control of batch crystallizers; many other examples exist in the literature [7–9]. Simon et al. [10] described the concept of endoscopy–stroboscopy (an imaging technology

* Corresponding author.
E-mail addresses: K.Powell@lboro.ac.uk (K.A. Powell), zknagy@purdue.edu (Z.K. Nagy).

http://dx.doi.org/10.1016/j.cep.2015.01.002

widely used in medical diagnostics) for on-line monitoring of a crystallization process. In a recent review, Nagy et al. [11] highlighted key research efforts in the application of PAT and information systems in the areas of process monitoring, modeling and control. On the subject of crystallization monitoring and control, the authors drew attention to recent developments in sensing hardware and processing algorithms, for example, the application of chemometrics and digital image processing techniques.

Although continuous crystallization is gaining popularity in both industrial and academic research laboratories, there are only a limited number of studies in the literature, and these mainly consider fine chemicals [12–17]. There are even fewer studies on the application of PAT and information systems to monitor continuous crystallizers [12,18–20]. Kouglous et al. [12] were among the first to demonstrate the application of FBRM and PVI (particle video imaging) to real-time monitoring and steady-state characterization of a single-stage continuous MSMPR crystallization process. More recently, Ferguson et al. [18] used FBRM and ATR-FTIR to monitor the anti-solvent crystallization of benzoic acid in a comparative study using a single-stage continuous MSMPR and a plug flow crystallizer (PFC). In their study, Hou et al. [19] used PVM and FBRM to characterize crystal size and shape properties and steady-state during the cooling crystallization of PCM in a single-stage continuous MSMPR. Simon and Myerson [20] assessed the feasibility of using a FBRM probe perpendicular to the flow for continuous on-line monitoring of a plug flow crystallizer.

Many investigators report problems such as encrustation on vessel walls, fouling on process equipment and blockage of transfer lines [17], particle settling and classification [21] and difficulty in adopting PAT on small scale plug flow crystallizers [22]. These problems present significant developmental challenges to the implementation of continuous crystallization processes at industrial scale. However, despite the many challenges associated with continuous crystallization compared to batch processes, there are more degrees of freedom in operation that can enable the creation of a wider range of product attributes [23]. In addition, continuous crystallization equipment can be significantly intensified leading to simplification of process scale-up, which is a significant advantage over batch processes [18]. In order to overcome the limitations of current continuous crystallization equipment, novel operating principles are required that lead to significant improvement in crystallization outcomes.

The work presented herein examines the application of a novel concept referred to as a periodic MSMPR flow crystallizer (PMSMPR). Unlike the conventional continuous MSMPR operation described by Randolph and Larson [24,25], in which product slurry is continuously withdrawn and has exactly the same composition as the vessel, the PMSMPR method of operation involves periodic transfer of slurry (addition and withdrawal) at high flow rates from either a single stirred vessel or between a number of stirred vessels arranged in series. The PMSPPR is therefore characterized by periodic withdrawal of product slurry. Similar to a continuous MSMPR, the product withdrawn during the PMSMPR operation has exactly the same composition as the vessel at the time of withdrawal. In PMSMPR operation, the rapid transfer of slurry at high flow rates prevents sedimentation and blockage of the transfer lines. The transfer of slurry is followed by an equilibration (or pause) period when no addition or withdrawal of slurry to/from the crystallizer vessel takes place, but the suspension continues to be agitated. The concept of periodic flow crystallization demonstrated here using the novel PMSMPR is different from intermittent addition/withdrawal methods reported recently [18,19], which involve the rapid addition/withdrawal of 10% or less of the crystallizer volume every one tenth of the mean residence time. Such a strategy was developed to enable the isokinetic withdrawal of slurry, and prevent transfer line blockage in “continuous” MSMPR crystallizers some years ago [26]. The PMSMPR used in this study was operated as a single- or two-stage unit, with and without a recycle stream to determine the effect on product CSD during PCM crystallization from isopropyl alcohol (IPA). Since seeding is an important aspect of crystallization, the effects of seed crystal properties on the product CSD were also investigated. During the process development stages feeding strategy, that is, constant versus intermittent feed supply was found to have an effect on the time to achieving a periodic steady-state operation (that is, “state of controlled operation” or SCO) and these results have also been presented as a significant finding.

The periodic flow process was monitored using an integrated array of PAT tools (ATR-UV/vis, Raman, PVM and FBRM) and an in-house developed crystallization process informatics systems (CryPRINS) software tool developed in LabView [27]. Temperature control on the process was implemented using thermostatic baths, linked to and controlled through CryPRINS.

Periodic flow operation offers a number of advantages compared to conventional continuous MSMPR methods. Due to rapid withdrawal from the crystallizer each period (or cycle), a more representative withdrawal of slurry is achieved. Conventional slurry addition/withdrawal methods use slow withdrawal rates that lead to the preferential removal of small crystals from the MSMPR. This phenomenon occurs due to the slower settling velocities and faster response times of small crystals compared to larger crystals [21]. Furthermore, the varied properties of crystals represented by a given CSD in the conventional MSMPR can lead to localized size distributions, in particular, where non-ideal mixing conditions predominate [21,28]. Such classification phenomena ultimately lead to instabilities (i.e., oscillations) in the CSD, in which case high withdrawal velocities help to achieve representative sampling. The effective control of slurry classification during addition/withdrawal can lead to a narrower CSD with larger mean crystal size.

A significant challenge associated with continuous crystallization processes involves the generation of nuclei for later growth. Often seed nuclei are generated in situ, which demands high levels of supersaturation to encourage primary nucleation. The problem with this approach is that heterogeneous primary nucleation dominates the process and can ultimately lead to encrustation, blockage of transfer lines, fouling on process equipment and the preferential removal of fines due to low flow rate and narrow transfer line requirements. Periodic flow crystallization is advantageous because the problems encountered in continuous flow crystallization are avoided completely when the crystallizer is operated as a seeded system at low supersaturation. Another advantage of period flow demonstrated in this study is the control over the mean residence time of fluid elements inside the crystallizer due to the incorporation of an equilibration or pause period in the operating cycle. For example, the mean residence time could be shortened or extended to control mean crystal size and distribution. The subsequent pumping period allows for rapid and representative transfer of slurry in this operation. Effectively, the periodic flow process is a hybrid system that combines the best aspects of batch and continuous stirred tank crystallization, that is, long residence time and constant flow of materials.

2. Materials and methods

2.1. Basic experimental setup

The cooling crystallization of PCM (4-acetaminophenol, 98% purity purchased from Sigma–Aldrich, UK) from a solvent, isopropyl alcohol (IPA) (propan-2-ol, analytical reagent grade, 99.97% purchased from Fisher Scientific, UK), was investigated

using a PMSMPR crystallizer unit. A batch system was also configured and used to conduct studies under similar conditions to those used for the PMSMPR study. The overarching aim of the studies conducted was to demonstrate as proof of concept, the potential benefits of periodic flow cooling crystallization using a PMSMPR. Another important aim was to determine the experimental conditions under which crystal growth could be achieved and secondary nucleation suppressed under periodic flow operation, i.e., the objective was to produce large crystals. A further aim was to demonstrate how PAT tools could be applied to determine when the periodic flow process achieves a "state of controlled operation" (SCO). Fig. 1 shows a schematic representation of the single-stage PMSMPR unit with a recycle stream. Also shown are the integrated PAT array and CryPRINS software that were used to monitor the process and control temperatures in each of the seeded cooling crystallization experiments. Temperature control of each vessel was achieved using individual thermofluid circulator baths (Huber Ministat 230) each controlled using a proportional integral (PI) feedback control mechanism.

A partial least square (PLS) calibration model was developed using Raman spectral data for real-time in situ concentration measurement of PCM in the liquid phase inside each crystallizer. Spectral pre-processing was done using a standard normal variate (SNV) transformation, followed by model-building based on the first derivatives of the spectral data. The model was validated using external standards and an ATR-UV/vis model previously developed by Saleemi et al. [29] The maximum error between the predicted and model determined concentration for the validation data set was 3.7%.

All experiments were carried out in jacketed glass vessels, fitted with PTFE lids with ports for the insertion of an overhead 4-pitched blade PTFE impeller, thermocouple, FBRM, Raman and PVM. Probes were inserted at appropriate positions, 2–3 cm above the impeller in each vessel for optimum process monitoring and temperature control. Dip tubes were positioned 1–1.5 cm above the impeller in each vessel (and below the probe tips). The pitch blade impellers in each vessel were positioned approximately 1.5 cm from the bottom. The stirrer speed was set to 300 rpm in each 500 mL PMSMPR. Each vessel, including the seeded feed vessel was continuously stirred during each experimental run using the overhead pitch blade impellers. The approximate power per unit volume from the selected impeller speed was 0.056 kW/m^3. Hou et al. [19] conducted a series of investigations to determine the agitation rate required to give homogeneous suspensions of PCM–IPA–H_2O system in a 530 mL continuous MSMPR. The study showed that impeller speeds ranging from 200–400 rpm (power output per unit volume ranged from 0.0186–0.1486 kW/m^3) produced homogeneous suspensions as confirmed by FBRM measurements from the top, center and bottom of the continuous MSMPR. It is well known that for isokinetic withdrawal of slurry from MSMPR to be achieved, there is a requirement to maintain a homogeneous suspension in the crystallizer. There are also further requirements for high flow rate and optimal positioning of the outlet dip tube to ensure rapid and representative slurry withdrawal.

2.2. Periodic flow crystallization experiments

Periodic flow crystallization experiments were carried out using the apparatus described in Fig. 1. The unit was reconfigured as required to operate either as a single-stage or two-stage PMSMPR, with and without a dissolver/recycle stream. Fig. 2 shows the process flow diagrams of the different PMSMPR configurations used during the study. Also shown are the mass flow rates, Q (i.e., of slurry) employed as well as the operating temperature and supersaturation (S) of each stage. S is the supersaturation ratio defined as c_o/c^*, where c_o is the initial solute concentration of the feed or PMSMPR and c^* is the equilibrium concentration at the specified operating temperature. A 5 L vessel was used to deliver seed suspension to the first stage PMSMPR. Masterflex® pumps operated in time dispense mode and platinum cured tubing (3.1 mm ID) were used for suspension transfer between vessels and from the PMSMPR to the filtration unit. Details of the start-up and operating procedures employed during the periodic flow crystallization experiments in the single- and two-stage PMSMPR units are outlined in Sections 2.2.1–2.2.3.

2.2.1. Seed preparation

To determine the effect of seed quality on the crystallization outcome, seed crystals were prepared in two ways:

(1) Sieving PCM raw material to within the size range 100–125 μm (referred to as "raw material seed"); and
(2) Sieving recrystallized PCM to within the size range 75–125 μm (referred to as "recrystallized seed").

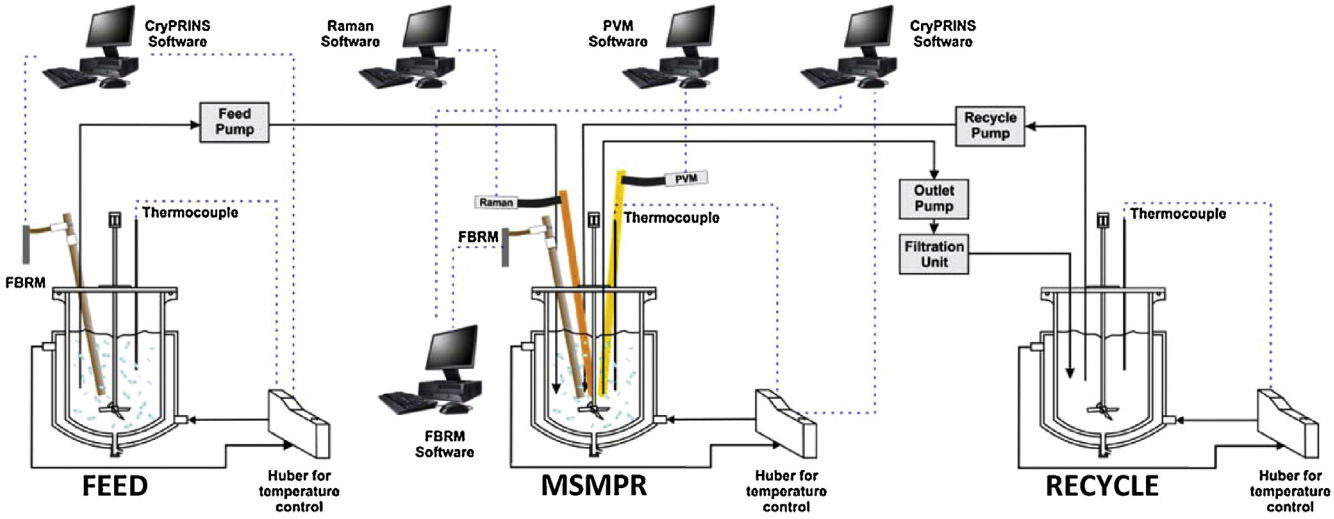

Fig. 1. Schematic of PMSMPR crystallizer used for the periodic flow crystallization experiments.

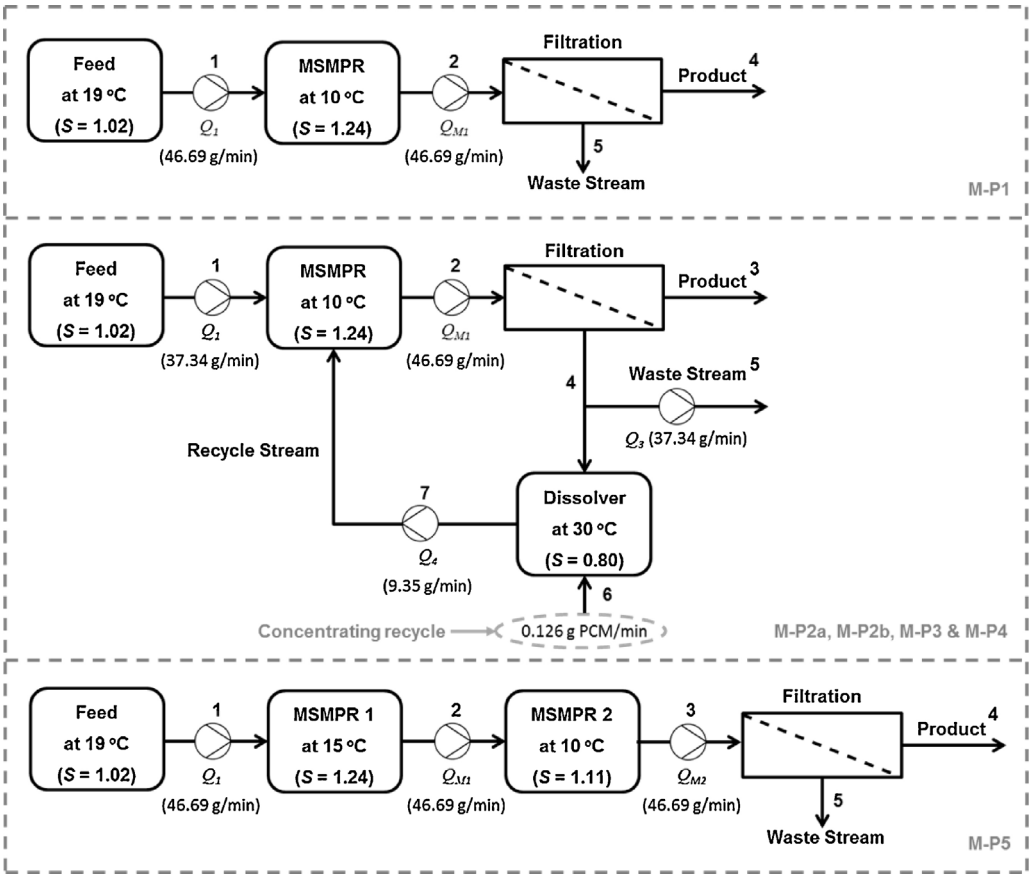

Fig. 2. Flow diagram showing the block configurations of the PMSMPR units used during the periodic flow crystallization study. M-P1 is a single-stage unit operated without recycle stream; M-P2a, M-P2b, M-P3 and M-P4 are all single-stage units operated with recycle stream. M-P5 is a two-stage unit operated without recycle stream.

2.2.2. Single-stage PMSMPR crystallization without recycle (M-P1)

The process flow diagram of the experimental set-up used for the single-stage PMSMPR experiment is shown in Fig. 2. Prior to start-up a fresh feed solution saturated at 20 °C (0.110 ± 0.002 g PCM/g IPA) was prepared in the 5 L feed vessel. The feed solution was then cooled to 19 °C, seeded with 2.5% (11.19 g) recrystallized seed and held for 30 min to give the crystals time to heal by Ostwald ripening [30]. The supersaturation of the feed stream to the PMSMPR was 1.02. At start-up, the single-stage PMSMPR was cooled to 10 °C, thereafter, feed suspension was added to give a final operating volume of 500 mL. This was then followed by an equilibration period of 10.64 min. Thereafter, a period of simultaneous addition of feed (at a rate of 46.69 g/min) to, and withdrawal of slurry (at a rate of 46.69 g/min) from the PMSMPR was initiated for a period of 9.36 min. The slurry withdrawn from the PMSMPR was filtered and the product crystals collected and dried at 40 °C for 24 h. The periodic addition/withdrawal and equilibration cycles were continued for the duration of the experiment. The equilibration cycle refers to that time period during which the pump are switched off and there is no net inflow of feed or outflow of slurry to or from the PMSMPR. The sum of the addition/withdrawal time period (9.36 min) and the equilibration period (10.64 min) is defined as the mean residence time (RT) of the single-stage PMSMPR (20 min).

2.2.3. Single-stage PMSMPR crystallization with recycle (M-P2a, M-P2b, M-P3 and M-P4)

For these experiments, the feed preparation and seeding procedure was the same as that described for the single-stage PMSMPR without recycle (M-P1) in Section 2.2.1. The single-stage PMSMPR configurations with recycle M-P2a, M-P2b, M-P3 and M-P4 were operated as follows:

M-P2a and M-P2b: seeded with raw material seed and operated with a non-concentrated recycle stream, that is, without the use of stream 6 as shown in Fig. 2.

M-P3: seeded with recrystallized seed and operated with a non-concentrated recycle stream, that is, without the use of stream 6 as shown in Fig. 2.

M-P4: seeded with recrystallized seed and operated with a concentrated recycle stream, that is, using stream 6 as shown in Fig. 2.

The start-up procedure for each of the single-stage PMSMPRs with recycle stream involved cooling the PMSMPR vessel to 10 °C followed by addition of feed suspension to a final volume of 500 mL. This was then followed by an equilibration period of approximately 10.64 min. Thereafter, a period of simultaneous addition of feed (at a rate of 46.69 g/min) to and withdrawal of slurry (at a rate of 46.69 g/min) from the PMSMPR was initiated for a period of 9.36 min. The slurry withdrawn from the PMSMPR was filtered rapidly and the filtrate solution added to the recycle vessel, which was kept at 30 °C to dissolve any fines present. Once sufficient filtrate was collected, the periodic addition and withdrawal operation of the PMSMPR was continued, but with an adjustment of flow rate from the feed stream to the PMSMPR, that is, reducing from 46.69 to 37.34 g/min. This was done to compensate for the additional inlet flow from the recycle stream at a rate of 9.35 g/min. To investigate the effect of recycle stream supersaturation level on the crystallization outcome, two methods of recycle were investigated:

(1) Non-concentrated whereby filtrate solution was added directly to the PMSMPR after filtration and dissolution; and

(2) Concentrated whereby PCM raw material was added to the filtrate solution to increase the concentration level to the equilibrium concentration of the feed stream.

The experiment with concentrated recycle (M-P4) was designed to investigate the effect on process yield. For this study, the filtrate liquor collected from the waste stream of the experiment carried out with non-concentrated recycle stream (M-P3) was weighed and the concentration determined by ATR-UV/vis (0.104 ± 0.001 g PCM/g IPA). The filtrate liquor was then concentrated to the equilibrium concentration of the feed stream liquor entering the PMSMPR. The overall rate of addition of PCM to the recycle stream was estimated at 0.126 g/min as shown in Fig. 2. The concentrated recycle stream liquor was added to the PMSMPR at a rate of 9.35 g/min. The operating principle of M-P2a, M-P2b and M-P4 was the same as described for M-P1 in Section 2.2.2.

2.2.4. Two-stage PMSMPR crystallization without recycle (M-P5)

Fig. 2 shows the process flow diagram of the two-stage PMSMPR crystallizer set-up used. The feed preparation and start-up procedure was similar to that employed for the single-stage PMSMPR study without recycle (M-P1), except that an additional PMSMPR vessel was used. At start-up the first and second stage PMSMPR vessels were cooled to 15 and 10 °C respectively. Seed suspension was then pumped from the feed vessel to the first stage PMSMPR filling it to the desired working volume of 500 mL. This was followed by an equilibration period of 10.64 min. Following this, the pumps from the feed vessel to the first stage and from the first stage to the second stage PMSMPR were switched on simultaneously for 9.36 min. This procedure allowed sufficient time for one working volume of the first stage to be transferred to the second stage. Following this, there was an equilibration period of 10.64 min. Thereafter, the pumps for all transfer lines were operated periodically over the time intervals mentioned until the end of the experiment. Slurry withdrawn from the second stage PMSMPR vessel each period was filtered and the crystals collected and dried for off-line microscope image analysis. The sum of the addition/withdrawal time period (9.36 min) and the equilibration period (10.64 min) for each stage of the two-stage PMSMPR is defined as the mean RT, which is 40 min.

2.2.5. Batch crystallization experiment B-C1

A seeded batch cooling crystallization experiment was conducted for comparison with, and further characterization of the PMSMPRs. At start-up a suspension of 0.109 g PCM/g IPA was dissolved at 30 °C (10 °C above the desired saturation temperature) in a 500 mL vessel and held for 15 min. The solution was then cooled to 19 °C, seeded with 2.5% PCM seed and held for 30 min. The resulting seed suspension was then cooled to 10 °C and held for 423 min. The batch crystallization experiment was used as a mean of examining further some of the crystallization phenomena observed in the PMSMPRs.

2.2.6. Summary of experimental conditions

Table 1 gives a detailed summary of the experimental conditions used for each of the batch and PMSMPR cooling crystallization experiments conducted during the study.

3. Results and discussions

3.1. Periodic flow crystallization

Several challenges were encountered during the development stages of a continuous MSMPR crystallizer unit for the crystallization of PCM from IPA, which included: encrustation, fouling on the walls of the process equipment and transfer tubes and blockage of transfer lines. A novel strategy for the crystallization of PCM involving periodic mixed suspension removal was developed, which leads to the illustration of the concept of "state of controlled operation". Unlike intermittent operating procedures reported in the literature [18], periodic mixed suspension removal involves simultaneous addition and withdrawal of slurry from a stirred tank crystallizer at high flow rates and over a fixed time period. This is then followed by an equilibration or pause period during which time the system is allowed to stay undisturbed until the next addition and withdrawal cycle. This type of operation involves alternating periods of true continuous and batch operations, hence the mean residence time of crystals in the case of periodic operation (RT_{PO}) can be extended with the duration of batch operation period (t_{batch}), $RT_{PO} = RT_{conti} + t_{batch}$). The periodic flow method of operation has two main advantages:

Table 1
Summary of experimental conditions used for the cooling crystallization of PCM in the PMSMPR crystallizer.

Experimental conditions	M-P1	M-P2a	M-P2b	M-P3	M-P4	M-P5	B-C1
Feed temperature (°C)	19	19	19	19	19	19	n/a
PMSMPR temperature (°C)	10	10	10	10	10	(15; 10)*	n/a
Dissolver temperature (°C)	n/a	30	30	30	30	n/a	n/a
Feed concentration (g/g)	0.110	0.112	0.110	0.111	0.111	(0.110; 0.096)**	n/a
PMSMPR/crystallizer steady-state supersaturation (c/c^*)	1.17	1.16	1.15	1.18	1.15	(1.20; 1.09)***	1.25
Seed loading (%): raw material+	n/a	2.5	2.5	n/a	n/a	n/a	n/a
Seed loading (%): recrystallized material++	2.5	n/a	n/a	2.5	2.5	2.5	2.5
Periodic flow rate: feed stream, Q_1 (g/min)	46.69	37.34	37.34	37.34	37.34	46.69	n/a
Periodic flow rate: MSMPR1 outlet, Q_{M1} (g/min)	46.69	46.69	46.69	46.69	46.69	46.69	n/a
Periodic flow rate at MSMPR2 outlet, Q_{M2} (g/min)	n/a	n/a	n/a	n/a	n/a	46.69	n/a
Periodic flow rate of recycle stream, Q_4 (g/min)	n/a	9.35	9.35	9.35	9.35	n/a	n/a
Recycle ratio (Q_4/Q_1)	n/a	0.25	0.25	0.25	0.25	n/a	n/a
Addition and withdrawal period (min)	9.36	9.36	9.36	9.36	9.36	9.36	n/a
Equilibration period (min)	10.64	10.64	10.64	10.64	10.64	10.64	n/a
Mean RT (min)	20	20	20	20	20	40	423
Masterflex tube size (mm ID)	3.1	3.1	3.1	3.1	3.1	3.1	n/a

M-P1: Periodic flow single-stage MSMPR without recycle stream (2.5% recrystallized seed); M-P2a and M-P2b: Periodic flow single-stage MSMPR with non-concentrated recycle stream (2.5% raw material seed); M-P3: periodic flow single-stage MSMPR with non-concentrated recycle stream (2.5% recrystallized seed); M-P4: periodic flow single-stage MSMPR with concentrated recycle (2.5% recrystallized seed); M-P5: periodic flow two-stage MSMPR without recycle (2.5% recrystallized seed); ()* temperature of 1st and 2nd stage MSMPR respectively; ()** concentration in 1st and 2nd stage MSMPR respectively; ()*** supersaturation in 1st and 2nd stage MSMPR respectively; +100–125 μm raw fraction; and ++75–125 μm fraction.

(1) For a seeded system, it allows for addition of seed suspension and representative and isokinetic withdrawal of product crystals; and
(2) Extends the RT (where $RT = RT_{PO}$) of slurry inside the MSMPR, which can lead to improved yield and larger product crystals.

In addition, issues such as fouling on process equipment, encrustation and blockage of transfer lines are avoided, particularly when operating at low supersaturation with seeding. These advantages allow an extended operating time, without interruptions that necessitate, for example, cleaning of PAT probes, transfer lines or vessel walls due to the issues mentioned earlier. Fig. 3a–f shows the process time diagrams for the periodic flow crystallization experiments conducted in the different PMSMPR configurations as shown in Section 2.2 and in the same order as shown in Table 1; a batch crystallization experiment is also shown in Fig. 3g for comparison. A description of each experiment is given in Sections 3.1.1–3.1.5 and 3.2.

3.1.1. Single-stage PMSMPR without recycle (M-P1)

The process time diagram for the single-stage PMSMPR experiment without recycle stream (M-P1) is shown in Fig. 3a.

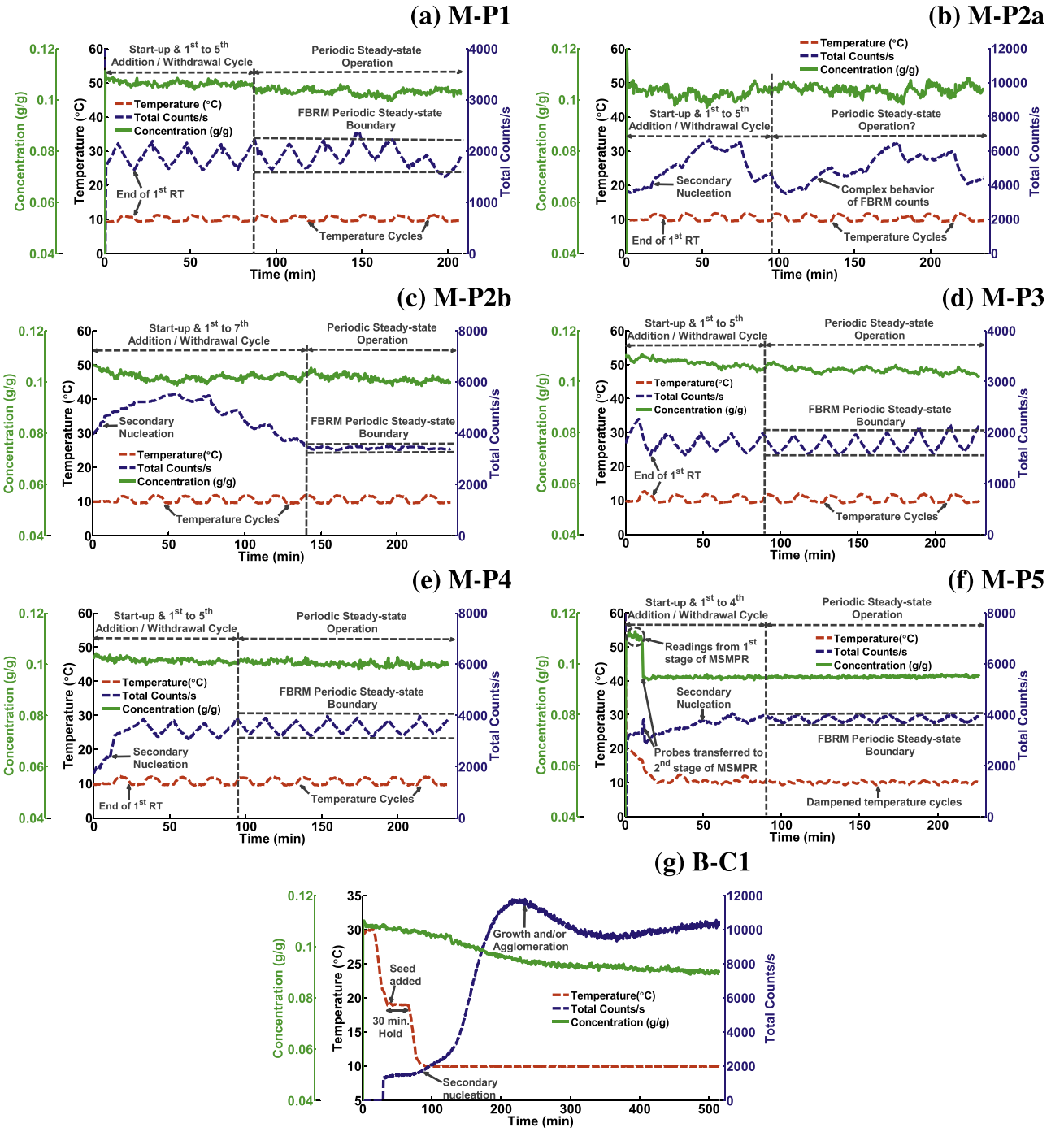

Fig. 3. Process time diagrams showing real-time temperature, FBRM counts/s and Raman concentration data for: (a) M-P1: single-stage PMSMPR, no recycle stream; (b) M-P2a and (c) M-P2b: single-stage PMSMPR, non-concentrated recycle; (d) M-P3: single-stage PMSMPR, non-concentrated recycle; (e) M-P4: single-stage, concentrated recycle; (f) M-P5: two-stage PMSMPR, no recycle stream; (g) B-C1: batch crystallizer.

The start-up period is rapid, leading to little rapid attainment of periodic conditions. The cyclic behavior of the concentration, temperature and FBRM counts data reflects the periodic mode of operation. Recrystallized PCM was used to prepare seed material used in the study. The concentration in the PMSMPR decreased gradually from start-up until the 5th addition/withdrawal cycle, to a steady-state value of 0.104 g PCM/g IPA ($S = 1.07$) as determined by Raman measurements. This was a result of the seed material rapidly consuming available supersaturation, primarily by promoting secondary nucleation, but also through growth on the surface of any crystals already present. Thereafter, the concentration change was only small after the 5th addition/withdrawal cycle (marked by the vertical dashed line in Fig. 3a). A periodic steady-state operating region is shown in Fig. 3a, where the concentration changes only by less than 3%. A periodic steady-state boundary (±270 counts/s around an average value of 1890 counts/s) is also shown for the FBRM counts. The concept of periodic steady-state has not yet been defined in the literature in reference to MSMPR crystallization. Here it refers to that state of the system which maintains itself despite transitory effects caused by periodic disruptions. The FBRM counts/s, concentration and temperature data from Fig. 3a–f also gives an insight into the effect of periodic operation on the particle properties and supersaturation level of the system. During each equilibration or pause cycle there is a slow but sustained increase in the number of particles detected by FBRM, because of secondary nucleation, which results from a rapid generation of supersaturation (the average is around $S = 1.24$) in the PMSMPR (feed stream cooled rapidly from 19 to 10 °C) leading to an increase in crystal density. On the other hand, during each addition/withdrawal cycle, there is a decrease in the FBRM counts/s, which is indicative of a reduction in crystal density; slurry is withdrawn from the PMSMPR and dilution occurs due to addition of fresh feed. The system is most affected by dilution with fresh feed suspension ($S = 1.02$) due to the higher temperature (19 °C) relative to the PMSMPR (10 °C). Initially, this leads to a reduction in the local supersaturation in the PMSMPR, which then leads to suppression of secondary nucleation. Once the addition/withdrawal cycle ends and the equilibration cycle (or pause period) begins, the suspension starts to cool more rapidly generating supersaturation, which leads to an increase in secondary nucleation in the system. It appears that for PCM, secondary nucleation is the dominant crystallization mechanism under the operating conditions employed. However, it appears that due to the periodic operation, the extent of secondary nucleation is controlled.

Evidence of this is drawn from the batch crystallization experiment (B-C1, Fig. 3g) process time diagram, which shows that as the system starts cooling from 19 °C, there is a slow increase in counts, indicative of secondary nucleation. Once the system cools to the final operating temperature of 10 °C there is a rapid and sustained increase in counts, indicative of a rapid onset of secondary nucleation. With periodic operation, rapid sustained increase in nuclei is avoided and the system rapidly attains periodic steady-state operation due to simultaneous feed addition and slurry withdrawal.

3.1.2. Single-stage PMSMPR with non-concentrated recycle (M-P2a and M-P2b)

Fig. 3b and c shows the process time diagrams of the single-stage PMSMPR experiments with recycle stream, in which PCM raw material was used to prepare seed suspension in the feed

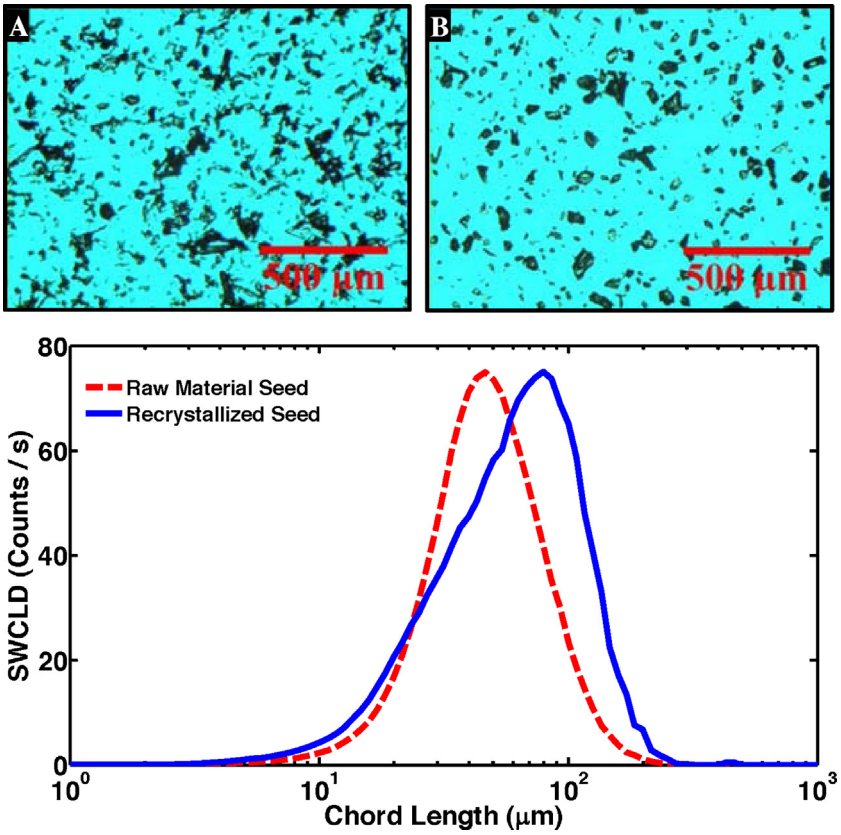

Fig. 4. Top: microscope images of dry seed crystals used in the periodic flow crystallization study: (A) seed from sieved PCM raw material (100–125 µm fraction); and (B) seed from sieved recrystallized PCM (75–125 µm fraction); below: comparison between FBRM SWCLDs for the seed materials prepared from PCM raw and recrystallized materials respectively.

vessel (M-P2a and M-P2b). M-P2a was one of a series of initial process development experiments conducted to investigate periodic flow operation of the single-stage PMSMPR and was carried out using a 1 L feed vessel as opposed to the 5 L feed vessel used for M-P2b and all subsequent PMSMPR experiments reported here. The process time diagram for M-P2a, (shown in Fig. 3b) indicates complex behavior of the FBRM counts/s data and it appears that a periodic steady-state (that is, a state of controlled operation) has not been achieved. In contrast, the Raman concentration data indicates a decrease in concentration during the start-up phase, which then stabilizes from the 5th addition/withdrawal cycle (as shown in Fig. 3b) to a periodic steady-state (average 0.102 ± 0.002 g PCM/g IPA) until the end of the experiment. The FBRM counts/s data result from an operating weakness in this initial PMSMPR crystallizer design: the use of the 1 L tank to supply the seed slurry to the PMSMPR in M-P2a experiment may have led to variations in the mass fraction of seed crystals delivered; the 1 L tank had to be refilled periodically to continue supplying feed suspension to the 500 mL PMSMPR. For each refill, a fresh batch of saturated solution (1.2 L) in a separate vessel and cooled to 19 °C. This solution was then added to the feed tank, followed by addition of dry seed crystals (2.5%) to make the seed slurry. In contrast, the 5 L tank used in M-P2b experiment (Fig. 3c) provided a more consistent supply of feed suspension since only a single preparation of saturated solution and seed crystals was necessary. Moreover, the longer residence time of slurry in the 5 L feed tank, allowed for aging of the seed crystals and surface healing via Ostwald ripening mechanism.

Fig. 4 shows the microscope images of PCM seed prepared from raw material (A) and recrystallized material (B), respectively. The images clearly show the varied size and shape properties of the former compared to the latter. The seed crystals prepared from recrystallized PCM were of better quality, showing more uniform size and shape crystals.

A fundamental limitation of the FBRM technique is that it measures chord lengths rather than true particle sizes; typically, a large number of chords of different sizes can be obtained from any given particle [27]. Furthermore, different intensity profiles are often obtained from crystals of different sizes and shapes. Therefore it is likely that in suspensions of crystals with a wide variety of morphologies, an even greater number of different chords may be obtained relative to a suspension of crystals with a more uniform shape. In addition, it is likely that the frequency of refilling the 1 L vessel used to supply feed to the 500 mL PMSMPR during the M-P2a experiment also contributed to variations in the FBRM counts. The periodic refilling with fresh feed may have caused non-uniform and therefore inconsistent transfer of seed suspension from the feed to the PMSMPR. This can be attributed to changes in mass fraction content of seed crystal in the feed suspension during discharge from the 1 L feed vessel due to: (1) slight variations that occurred in the seed slurry each preparation cycle; and (2) change in the properties of the seed slurry on refilling of the feed tank, due to small amounts of seed suspension leftover/accumulated from previous refill(s). A secondary factor that may have affected the properties of the seed slurry in the 1 L feed tank is insufficient time for the aging process and Ostwald ripening/healing of the seed crystal surface to take place.

In contrast, the process time diagram of experiment M-P2b in Fig. 3c shows a FBRM counts/s profile that can be more easily interpreted: there is an initial increase in FBRM counts from start-up due to secondary nucleation. The same phenomena can be observed in the time diagram for M-P2a experiment (Fig. 3b). However, in M-P2b the FBRM counts/s profile shows a steady, but sustained decrease in particle number until the 7th addition/withdrawal cycle, indicative of the occurrence of crystal growth and/or agglomeration in the system. From the 7th addition/withdrawal cycle onwards the counts/s measurements level off, except for the occurrence of dampened cycles due the periodic operation. In Fig. 3c, this is highlighted as the point of attainment of steady-state in M-P2b. This was also confirmed by the Raman concentration measurements, which showed steady-state behavior over the same time period. The change in concentration from the 7th RT to the end of the experiment was less than 4% (± 0.0041 g PCM/g IPA). The results from M-P2b experiment suggests that the most probable cause of the complex behavior of the FBRM counts/s data obtained from M-P2a experiment was the frequency of refilling the 1 L feed vessel. The results therefore indicate that selection of a stable and consistent feed delivery system is important from the perspective of attaining a steady-state particle count in the PMSMPR. It is also evident from both M-P2a and M-P2b that the FBRM counts/s in both systems at start-up is more than twice that observed for the experiments in which recrystallized seed material was used. The sieved PCM raw material seed contains many small particles in comparison to the recrystallized seed, as can be seen in the microscope images shown earlier in Fig. 4.

Another interesting observation from M-P2b is that the system takes a longer time to achieve periodic steady-state operation, compared to the other PMSMPR studies. This suggests that the seed properties have an effect on the time to achieving periodic steady-state operation. This is a reasonably straightforward phenomenon whereby the smaller sized seed material (SWMCL 49–50 μm) used in M-P2b (and M-P2a) is capable of consuming supersaturation more quickly compared to the recrystallized seed material (SWMCL 66–70 μm) used in the other PMSMPR experiments reported in this study. Since the time required to achieve steady-state depends on the kinetics of the crystallization process, faster growth can lead to smaller time constants. It is accepted in general, that smaller sized seeds exhibit larger overall active surface area thus higher active site concentration, which can lead to faster mean growth rates in an MSMPR exhibiting growth rate dispersion. The periodic steady-state product size of crystals from M-P2b was 67 μm. A steady-state crystal product size could not be determined for M-P2a. For experiment M-P2b, a periodic steady-

Table 2
Summary of experimental results for the cooling crystallization of PCM in the PMSMPR and batch crystallizers.

Parameters measured	M-P1	M-P2a	M-P2b	M-P3	M-P4	M-P5	B-C1
Mean steady-state crystallizer concentration, c_1 (g/g)	0.103	0.102	0.101	0.104	0.101	0.095	0.089
% Yield (i.e., fractional yield) of crystalline product	35.3 ± 1.9	43.3 ± 1.9	41.5 ± 1.1	31.1 ± 1.0	37.5 ± 0.5	68.9 ± 0.4	96.1 ± 0.1
Time to achieve steady-state operation (min/RT_{PO})	89.5/5th	n/a	140/7th	89.0/5th	90.0/5th	89.0/5th	460/n/a
Mean size of seed crystals: FBRM MSWCL (μm)	70.1 ± 0.1	48.7 ± 0.2	49.9 ± 0.7	70.1 ± 0.1	66.3 ± 0.1	70.1 ± 0.1	66.7 ± 0.2
Steady-state mean crystal size: FBRM MSWCL (μm)	74.5 ± 0.4	n/a	67.4 ± 0.3	71.5 ± 0.1	64.6 ± 0.1	77.7 ± 0.2	59.6 ± 0.1

M-P1: periodic flow single-stage MSMPR without recycle stream (2.5% recrystallized seed); M-P2a and M-P2b: periodic flow single-stage MSMPR with non-concentrated recycle stream (2.5% raw material seed); M-P3: periodic flow single-stage MSMPR with non-concentrated recycle (2.5% recrystallized seed); M-P4: periodic flow single-stage MSMPR with concentrated recycle stream (2.5% recrystallized seed); M-P5: periodic flow two-stage MSMPR without recycle stream (2.5% recrystallized seed); RTPO: mean residence time; and n/a: not applicable.

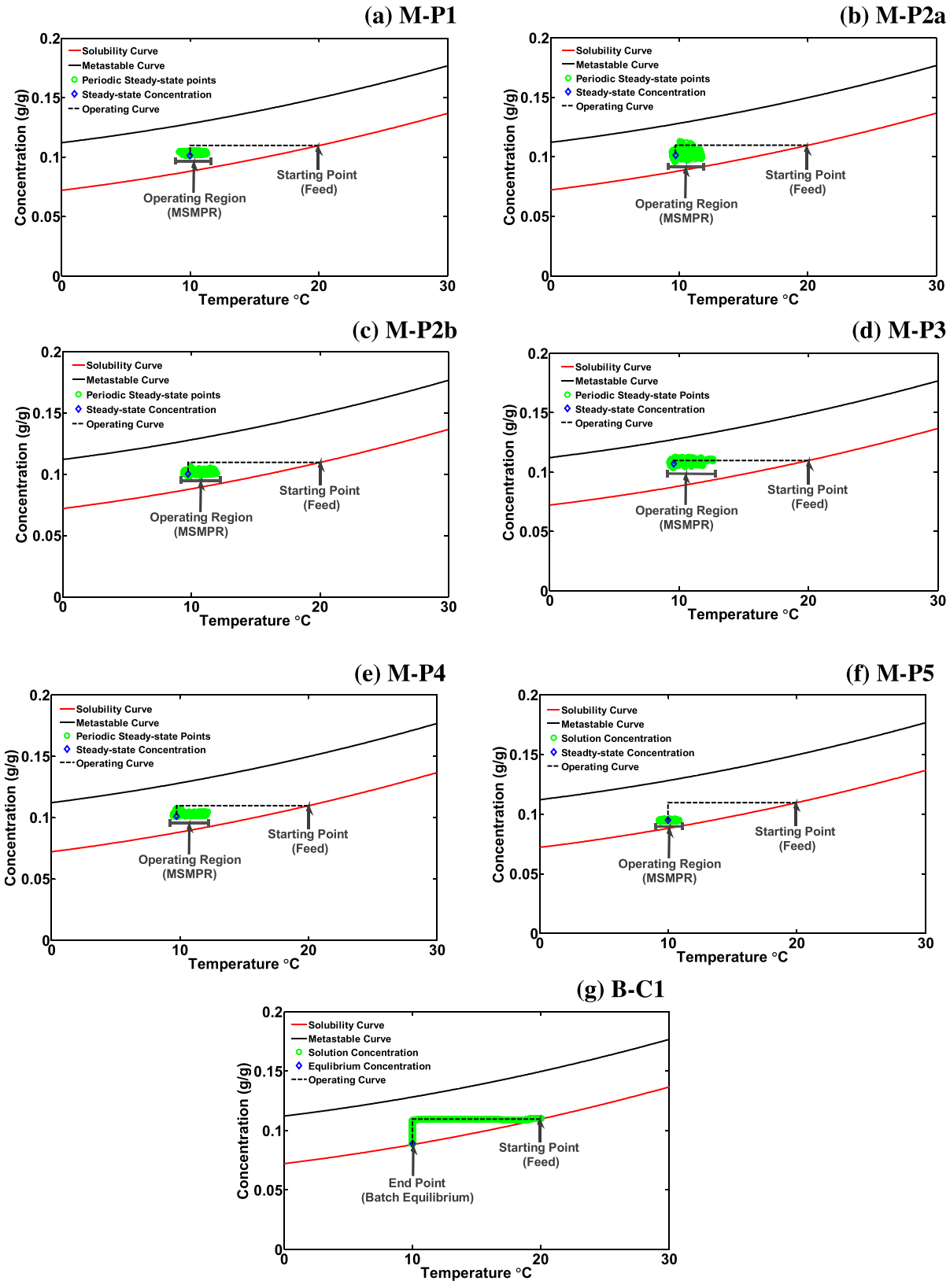

Fig. 5. Process phase diagrams for the PMSMPR and batch crystallization experiments showing operating region for each system: (a) M-P1: single-stage PMSMPR, no recycle stream; (b) M-P2a and (c) M-P2b: single-stage PMSMPR, non-concentrated recycle; (d) M-P3: single-stage PMSMPR, non-concentrated recycle; (e) M-P4: single-stage, concentrated recycle; (f) M-P5: two-stage PMSMPR, no recycle stream; (g) B-C1: batch crystallizer.

state boundary (±80 counts/s) for the FBRM counts is also shown in Fig. 3c. The FBRM cycles are significantly dampened over the steady-state period, indicating fewer disturbances to the particle properties of the system. This is an interesting observation and it indicates that the seed properties also have an effect on limiting the disturbances caused by periodic flow operation.

3.1.3. Single-stage PMSMPR with non-concentrated recycle (M-P3)

The process time diagram of the single-stage PMSMPR experiment with non-concentrated recycle stream (M-P3) is shown in Fig. 3d. The system rapidly achieves periodic steady-state operation after the 5th addition/withdrawal cycle. The initial concentration of (recrystallized PCM) seed suspension delivered to the PMSMPR was (0.111 g PCM/g IPA). The process concentration decreased from start-up until the 5th addition/withdrawal cycle to 0.104 g PCM/g IPA. Thereafter, the concentration decreased only marginally from the 5th addition/withdrawal cycle, marked by the vertical dashed line in Fig. 3d; periodic steady-state operating region was established and the concentration changes by less than 3%. A periodic steady-state boundary (±300 counts/s) is defined for the FBRM counts as indicated by parallel dashed lines in Fig. 3d.

3.1.4. Single-stage PMSMPR with concentrated recycle (M-P4)

The process time diagram (Fig. 3e) for the single-stage PMSMPR experiment with concentrated recycle stream (M-P4) shows that the system rapidly achieves a periodic steady-state condition after the 5th addition/withdrawal cycle, as indicated by the vertical dashed line. The concentration of the feed decreased from 0.111 g PCM/g IPA to 0.101 g PCM/g IPA by the 5th addition/withdrawal cycle in the PMSMPR and thereafter changes by less than 3%. The FBRM counts/s remained steady within a defined periodic steady-state boundary (±400 counts/s) from the 5th addition/withdrawal cycle to the end of the experiment, as shown in Fig. 3e. The amplitude of the FBRM cycles has increased when compared to the experiment conducted non-concentrated recycle stream (M-P3), an indication that secondary nucleation in the system has increased due to the higher supersaturation of the system.

3.1.5. Two-stage PMSMPR without recycle (M-P5)

The process time diagram of the two-stage PMSMPR without recycle and with recrystallized seed is shown in Fig. 3f. The system achieves a periodic steady-state condition after the 5th addition/withdrawal cycle in the second stage PMSMPR. The concentration of seed suspension delivered to the first stage PMSMPR was (0.111 g PCM/g IPA) and the feed concentration decreased to 0.109 g PCM/g IPA in the first stage and then to 0.095 g PCM/g IPA in the second stage PMSMPR. Fig. 3f shows the change in concentration and FBRM counts/s from 0 to 11 min in the first stage PMSMPR. The probes were then transferred to the second stage PMSMPR as indicated. The temperature cycles as shown in Fig. 3f are dampened compared to the previous experiments where the single-stage PMSMPR unit was used, indicating more efficient temperature control in the two-stage PMSMPR due to the smaller temperature difference (5 °C) between the feed and subsequent two stages. Fig. 3f further shows that periodic steady-state was rapidly achieved in the two-stage PMSMPR. Both the FBRM counts/s and the Raman concentration are stabilized from the 5th addition/withdrawal cycle (3rd RT) until the end of the experiment, with a variation of less than 2%. A periodic steady-state boundary (±190 counts/s) is also shown for the FBRM counts.

3.2. Batch crystallization

The batch crystallizer was operated as close as possible to conditions employed during the periodic flow crystallization experiments. Fig. 3g shows the process time diagram of the batch crystallization experiment (B-C1). At start-up, a suspension of 0.110 g PCM/g IPA was dissolved at 30 °C and maintained at that temperature for 10 min. The resulting solution was then cooled at a rate of 1 °C/min to 19 °C and seeded with 2.5% seed (prepared from recrystallized material). At this stage in the process, the FBRM counts increases from 0 to 1750 counts/s. The vessel was maintained at 19 °C for 30 min and then cooled at a rate of 1 °C/min to 10 °C. On cooling, the concentration starts to decrease and there is a simultaneous increase in FBRM counts, which occurs gradually until the system reaches 10 °C, at which point there is a dramatic increase in the counts/s due to secondary nucleation. The increase in counts continues until approximately 225 min into the process. Thereafter, the FBRM counts start to decrease and concentration continues to decrease, indicating that the system has entered a growth and/or agglomeration dominated phase. This is then followed by a period after approximately 460 min where the FBRM counts and concentration begin to stabilize.

The batch crystallization experiment gives some insights into the effect of periodic operation on the crystallization outcome. In the PMSMPR, the addition/withdrawal cycles inadvertently impose control over the secondary nucleation kinetics of the system. In contrast, the batch process is dominated by uncontrolled secondary nucleation in the early stages of the process, which ultimately leads to fine particles and a broad CSD. In the periodically operated PMSMPR there is greater control over the CSD due to suppression of secondary nucleation during the addition/withdrawal cycles. A discussion on the FBRM square weighted chord length distributions (SWCLD), which gives an indication of the CSD obtained from each of the crystallization experiments can be found in Section 3.3.3.

The batch process attains an equilibrium condition (close to the solubility curve), whereas MSMPR processes operate at steady-state at a fixed point in the metastable zone. Therefore, it is always possible to get a higher yield from a batch process compared to a continuous MSMPR operated under similar conditions. However, a continuous MSMPR can be operated closer to the solubility curve if the RT is extended. This is usually done by increasing the number of MSMPR stages (may prove impractical for systems with slow growth kinetics) or by using low flow rates. The former may lead to a significant increase in the number of crystallization process equipment and by extension the overall cost of operation, whereas the latter option leads to sedimentation and therefore classified slurry withdrawal and eventual blockage of transfer lines [17]. Periodic flow operation extends the RT of the MSMPR without the use of additional stages whilst also ensuring isokinetic withdrawal of slurry.

3.3. Comparison of crystallization methods

3.3.1. Product crystal size and overall process yield

In this section, the crystallization experiments discussed in Sections 3.1 and 3.2 will be compared. A summary of experimental results from each of the crystallization experiments is presented in Table 2.

The yield reported for each experiment is the fractional yield of crystallization (Y), which refers to the amount of product obtained from the crystallizer relative to the amount of available supersaturation. Y is therefore defined as:

$$Y = \frac{c_i f_0 + c_{R1} f_{R1} - c_1 f_1}{c_i f_0 + c_{R1} f_{R1} - c^* f_1} \times 100 \quad (1)$$

where c_i,c_1, c^* and c_{R1} are respectively, the feed stream concentration (g PCM/g IPA), PMSMPR periodic steady-state concentration, equilibrium concentration at the specified operating temperature, recycle stream concentrations (note that where the recycle stream is non-concentrated $c_{R1} = c_1$; otherwise c_{R1} is

calculated using a mass balance around the dissolver unit in Fig. 2). f_0, f_1 and f_{R1}, are the mass flow rates of IPA from the inlet, outlet, and recycle streams of the PMSMPR respectively, that is, based on time-averaged flow. Note that $f_0 = M_1Q_1$, $f_1 = M_{M1}Q_{M1}$ and $f_{R1} = M_4Q_4$ where M_i is the mass fraction of IPA in each flow stream i and Q_1, Q_{M1} and Q_4 are the total mass flow rates of the inlet, outlet and recycle streams respectively.

The data shown in Table 2 indicates that the configuration of the PMSMPR (single- or two-stage), seeding strategy and the use of recycle stream (concentrated or non-concentrated) can affect the crystallization outcome in terms of yield, mean crystal size and the achieve time to steady-state operation. The time taken to reach periodic steady-state in each PMSMPR experiment is more or less similar (90 min), with the exception of M-P2b (as discussed in Section 2.2.3). With respect to configuration, the highest yield ($68.9 \pm 0.4\%$) and mean crystal size ($77.7\ \mu m \pm 0.2\ \mu m$) is obtained from the two-stage PMSMPR without recycle stream (M-P5). Of the single-stage PMSMPR configurations, the largest mean crystal size ($74.5 \pm 0.4\ \mu m$) was obtained from the system without recycle stream (M-P1), which was marginally larger than the seed material ($70.1\ \mu m$) used. The process yield from M-P1 experiment was $35.3 \pm 1.9\%$. In comparison, the configuration with a non-concentrated recycle stream (M-P3) gave a marginally smaller mean crystal size of $71.5 \pm 0.1\ \mu m$ and an overall product yield of $31.1 \pm 1.0\%$. The single-stage PMSMPR configuration with concentrated recycle stream (M-P4) gave a higher yield of $37.5 \pm 0.5\%$. However, the mean crystal size was smaller ($64.6 \pm 0.1\ \mu m$) compared to the recrystallized seed material used ($66.3 \pm 0.1\ \mu m$) and products from experiments M-P1 and M-P3 for which the same seed material was used. This is an indication that concentrating the recycle stream improves the process yield, but leads to smaller crystals, because of additional secondary nucleation. In all of the PMSMPR experiments reported, there was evidence of growth of product crystals relative to the seed crystals used, except for M-P4 where the product crystals were marginally smaller than the seed material used. This suggests that concentrating the recycle stream leads to an increase in secondary nucleation in the system. The extent of crystal growth observed in the PMSMPR was marginal for all experiments based on the FBRM MSWCL data presented in Table 2, that is, with the exception of M-P2b where a significant increase in product crystal size ($67.4 \pm 0.3\ \mu m$) relative to the seed material ($49.9 \pm 0.2\ \mu m$) used is observed.

In the batch crystallization experiment, it is clear that the process yield is higher ($96.1 \pm 0.1\%$) and the product crystal size (59.6 ± 0.1) is smaller than that obtained from each of the PMSMPR experiments. The issue of crystal growth in the PMSMPR experiments relative to seed crystals used (matured for 30 min in a 5 L vessel) will be discussed further in Section 3.3.3.

The process yield of M-P2a and M-P2b ($43.3 \pm 1.9\%$ and $41.5 \pm 1.1\%$) were higher compared to M-P3 even though the experimental conditions were almost identical. The main reason for this difference is down to the properties of the seed materials used. M-P3 was seeded with recrystallized PCM seed (75–125 μm) while M-P2a and M-P2b was seeded with PCM raw material (100–125 μm). Although sieved to within a narrower size fraction, the size of the seed obtained from the raw material was much smaller as shown earlier in Section 3.1.2 (Fig. 4). This was due to the amorphous and powdery consistency of the raw material, which gave very fine crystals that had a tendency of sticking together, and hence were not broken up sufficiently during the sieving process. Aamir et al. [31] showed that the material used to prepare seeds can affect the quality of the seed produced (the compound investigated was potassium dichromate); seed prepared from sieving recrystallized material had a distinctive shape, uniform size and shape, and had fewer fine particles compared to seed prepared from sieving milled material. The higher process yield obtained from M-P2a and M-P2b is therefore attributed to the properties of the seed crystals used. The seed material prepared from PCM raw material has a large surface area due to the presence of many fine particles. Therefore, this fine seed is able to consume supersaturation and grow more rapidly than the larger recrystallized seed material used in the other experiments. However, small seeds can also promote secondary nucleation and agglomeration according to Fujiwara et al. [32] in their study on the control of batch cooling crystallization of PCM from aqueous seeded solutions. The investigators found that seeding the system with small seed crystals (less than 100 μm) resulted in the promotion of secondary nucleation and agglomeration leading to a product of varying sizes and broad CSD at 5% seed loading. On the other hand, seeding with large seed crystals (sieve sizes 125–250 μm and 250–350 μm) led to the suppression of secondary nucleation and agglomeration, resulting in product crystals of more uniform size and shape and hence a narrower CSD. However, a limitation with using large seed as shown in the study is the long batch times that are required before significant growth is observed (3–5 h). This would translate to impractically long residence times in the periodically operated PMSMPR. Furthermore, the use of large as opposed to fine seed as demonstrated in this study, may lead to only marginal growth in the PMSMPR.

3.3.2. Operating trajectories in the phase diagram

Fig. 5 shows the process phase diagrams for each of the PMSMPR and batch experiments conducted. Shown are the solubility (Saleemi et al. [29]) and indicative metastable curves, operating curve (showing trajectory through the phase diagram), concentration readings from the process (that is, periodic steady-state points for each PMSMPR and solution concentration points for the batch crystallization), and the mean periodic steady-state concentration (PMSMPR)/equilibrium concentration (batch) points. The results show that the dynamics of batch and PMSMPR crystallization are markedly different, both giving different trajectories through the phase diagram. Since supersaturation is the driving force for crystallization, variations in the supersaturation trajectory can allow for the exploitation of more crystal attributes in terms of size [18], shape, distribution and polymorphic form. This observation is particularly true for the PMSMPR crystallizer.

MSMPR crystallizers are usually operated continuously or in this study periodically, and at steady-state, which means there is no progression in terms of time or spatial position. This means that the system is operated at a fixed supersaturation, which is

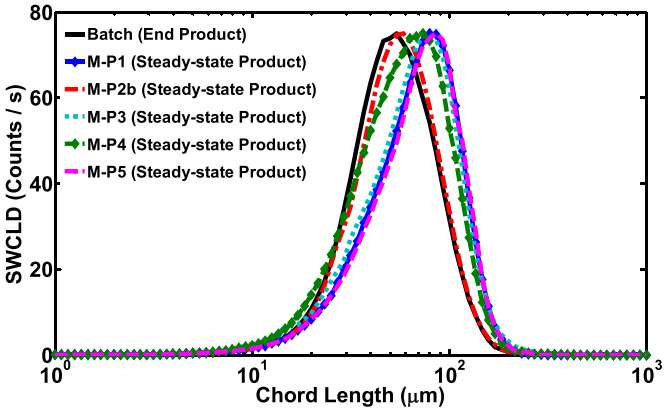

Fig. 6. Comparison between FBRM SWCLDs for the PMSMPR steady-state products and batch crystallizer end stage product.

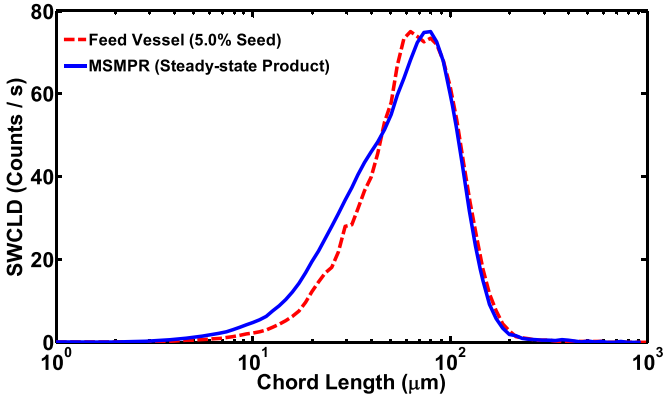

Fig. 7. Comparison between SWCLD of seed material (5.0%) and PMSMPR steady-state product.

also the point at which slurry is removed from the crystallizer. Compared to batch crystallization, which operates toward an equilibrium there is no supersaturation continuum in the MSMPR. However, if the MSMPR is operated periodically as done in this study then the supersaturation is no longer fixed, but oscillates periodically between a upper and lower limit values. So long as the oscillations are small, the system can be controlled as shown in this study to maintain a narrow supersaturation limit range (controlled state of operation). The phase diagrams for each of the PMSMPR experiments (Fig. 5a–f) show the effect of periodic operation as the system is disturbed at set time intervals due to slurry addition/withdrawal. However, the system approaches a periodic steady-state condition rapidly as the supersaturation boundaries narrow. It is also evident from the phase diagrams that the process yield from each PMSMPR is lower than that of the batch crystallization process. M-P5 (two-stage PMSMPR, recrystallized seed) shows the least variation in steady-state concentration (measurements from second stage PMSMPR) of all the PMSMPR operations. This is because of better temperature control due to the smaller temperature difference (5 °C) between stages, when compared to the single-stage PMSMPRs (9 °C difference from the feed vessel). Of the single-stage PMSMPRs, M-P1 (single-stage without recycle stream) shows the least variation in concentration in the operating region of the phase diagram, this is attributed to the absence of a recycle stream in this experiment. All of the single-stage PMSMPR experiments employing a recycle stream showed more variation in concentration due to the additional inlet flow creating slightly more

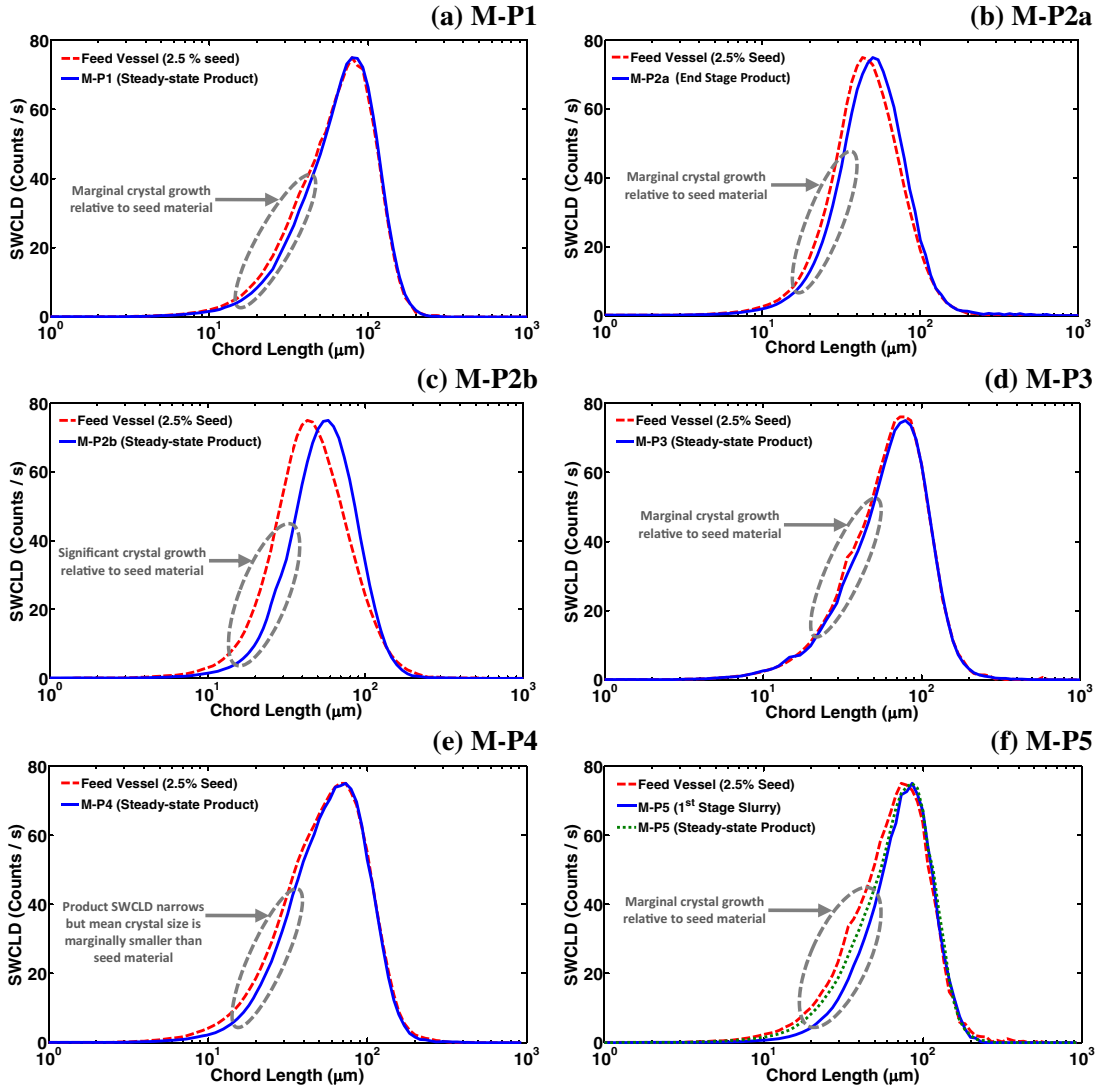

Fig. 8. Comparison between FBRM SWCLD for seed material and PMSMPR steady-state products, and seed material and batch crystallizer end stage product.

disturbance in the system. Furthermore, this additional inlet flow from the recycle stream, is at a lower supersaturation (S ranges from 0.75–0.80) and higher temperature (30 °C) relative to the feed stream (S = 1.02, at 19 °C) and PMSMPR (S = 1.24, at 10 °C). These differences in supersaturation also contribute to greater disturbance seen in each of the systems employing the recycle stream. However, these disturbances are maintained with reasonably narrow bounds so that the operation is still being controlled in a specific region of the metastable zone.

The merits of PMSMPR compared to continuous MSMPR have already been outlined. There also exists a significant potential with this mode of operation to explore different regions in the phase diagram and to determine the effect on crystallization outcomes in terms of product crystal attributes.

3.3.3. Comparison of FBRM distributions

Fig. 6 shows the normalized FBRM SWCLD of the final products obtained from the batch crystallization experiment and the steady-state products from the PMSMPR crystallization experiments. Compared to the batch experiment, all the distributions obtained for the PMSMPR experiments are shifted to the right (toward larger sizes). The distributions for M-P1, M-P3 and M-P5 are quite similar and appear to overlay, indicating that the product crystals are of similar mean size, in agreement with the SWMCL data reported in Table 2. The similarity between the steady-state product SWCLDs for M-P1, M-P3 and M-P5 also indicates that the number of stages employed (single- or two-stage) and the mode of operation (with or without recycle) do not have a significantly effect on the CSD in the PMSMPR. This is an interesting observation, since typically one would expect that an increase in the number of stages would lead to longer RT and significantly more time for crystals to grow. It must be noted, however, that although the distributions are similar for M-P1, M-P3 and M-P5, there is a very small but notable shift toward larger sizes in the two-stage PMSMPR (M-P5). Overall, the results suggest that the growth and secondary nucleation kinetics of PCM are the main variables affecting the crystallization. It appears that the secondary nucleation kinetics of the system is the dominant crystallization mechanism, while the growth kinetics is extremely slow. This was noticed early on in development studies in a seeded continuous MSMPR crystallizer.

A strategy was developed employing low supersaturation and moderate seed loading (2.5%) in the PMSMPR. Typically, seed loadings used in crystallization processes range from as little as 0.1% to as much as 5% and even more depending on the requirements [33]. Although each of the PMSMPRs were operated at low supersaturation with moderate seed loading, this strategy did not lead to significant crystal growth, with the exception of the M-P2b experiment where significant growth appears to have occurred due to the larger surface area of the seed material used. It is well known that low seed loading can contribute to undesirable secondary nucleation, leading to an increase in the number of small particles in solution [34]. Therefore, an investigation of periodic flow crystallization in the single-stage PMSMPR without recycle at a higher seed loading (5%) was conducted to determine the effect on the product crystal properties. Fig. 7 shows a comparison between the SWCLD of the seed and product crystals from this experiment.

The results indicate that even at a higher initial seed loading level, secondary nucleation is still having an effect on the product CSD. It is also likely that due to the high density of crystals in the system the competition for solute molecules is sufficiently high that the product crystals show no noticeable increase in size. The mean size of seed and steady-state product crystals, that is, the SWMCL observed for this experiment were 66.2 ± 0.3 μm and 61.8 ± 0.4 μm. The marginally smaller size of the product crystals relative to the seed crystals used affirms the deductions made earlier regarding the effect of secondary nucleation and competition for solute molecules. The results further confirm that the growth kinetics of PCM is extremely slow, whereas the secondary nucleation kinetics is much faster. Therefore, secondary nucleation may be the dominant crystallization mechanism.

Fig. 8 shows the normalized FBRM SWCLD of product crystals relative to the initial seed crystal distributions for the PMSMPR experiments. Evidently, only marginal crystal growth is observed

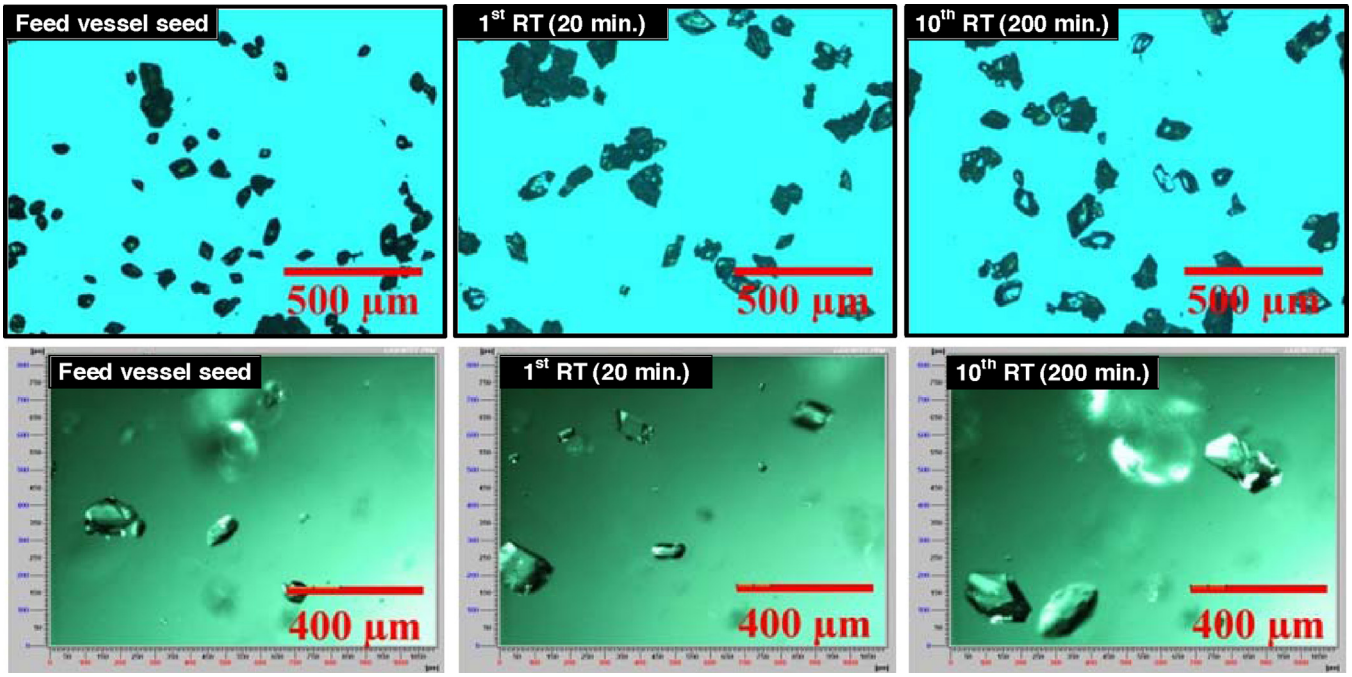

Fig. 9. Microscope (first row) and PVM images (second row) of seeds crystals from feed stream, and crystals from the 1st RT (20 min) and 10th RT (200 min) of the single-stage PMSMPR operated without recycle stream (M-P1).

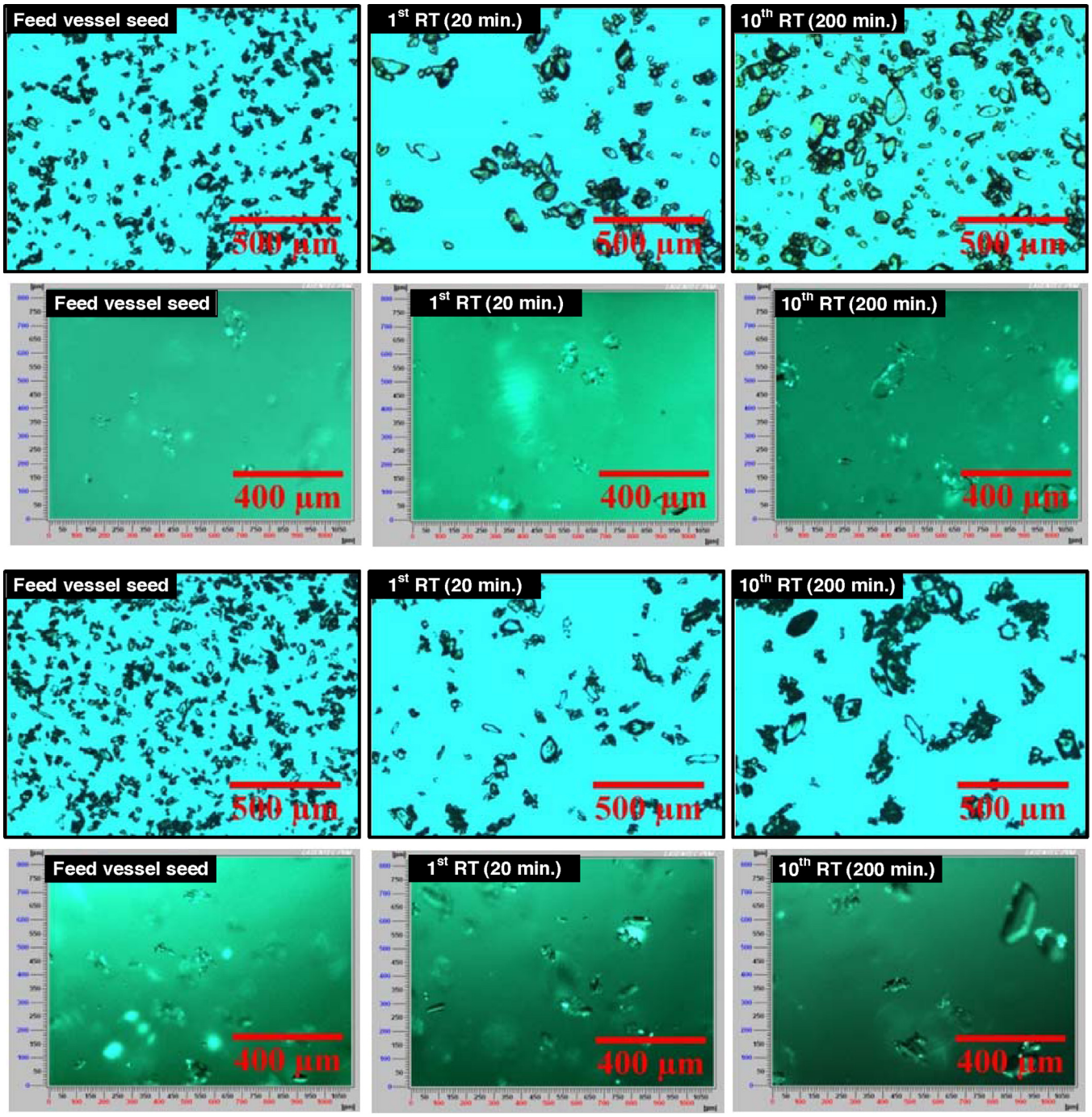

Fig. 10. Microscope (first and third rows) and PVM images (second and fourth rows) of seeds crystals from feed stream, and crystals from the 1st RT (20 min) and 10th RT (200 min) of the single-stage PMSMPR operated with non-concentrated recycle stream, M-P2a (top 2 rows) and M-P2b (bottom two rows).

relative to the seed crystals used for M-P1, M-P3 and M-P5 respectively. This is indicated by a narrower SWCLD compared to the seed crystals. However, for M-P4 the product crystals obtained from the PMSMPR were marginally smaller than the seed crystals. Interestingly, the product crystal SWCLD for M-P4 was narrower than that of the seed crystals, though the mean crystal size is smaller. For the batch experiment (B-C1) the product crystal SWCLD (not shown) showed a significant shift to the left and was significantly broadened relative to the seed size distribution, which is a further evidence that secondary nucleation is the dominant crystallization mechanism for PCM. Overall the results indicate that the PMSMPR produces marginally larger crystals with narrower CSD when compared to seed crystals used. PCM is known to exhibit slow growth crystallization kinetics [32] and may require longer RT and much narrower temperature transitions between process vessels to achieve significant crystal growth. The authors are currently investigating the optimization of the periodic flow crystallization conditions using a combination of mathematical modeling and experimental work to identify conditions suitable for growth of PCM. It is already evident from the results of M-P5 (two-stage PMSMPR) experimental run that the crystal size increases by extending the residence time in the

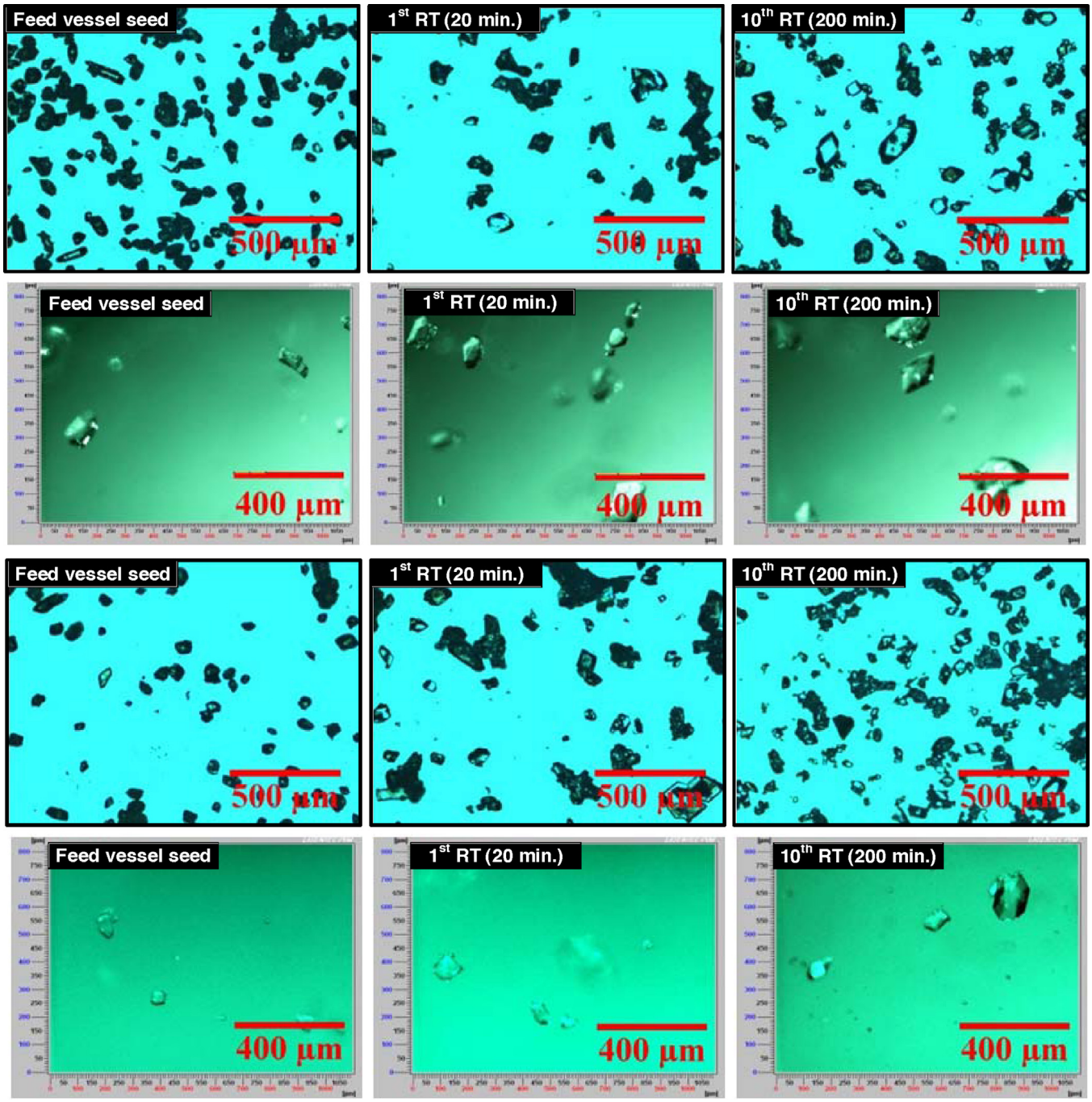

Fig. 11. Microscope (first and third rows) and PVM images (second and fourth rows) of seeds crystals from feed stream, and crystals from the 1st RT (20 min) and 10th RT (200 min) of the single-stage PMSMPR operated with non-concentrated (M-P3, top two rows) and concentrated (M-P4, bottom two rows) recycle stream.

PMSMPR simply by numbering up stages in a cascade, which has the added advantage of applying more gradual temperature changes transitions. This allows for smaller changes in supersaturation, which is more suitable for slow growing systems [15]. Preliminary experiments in the PMSMPR unit with a fast growing system showed that significant growth of product crystals was achieved relative to seed crystals when compared to PCM, which further indicates that the slow growth kinetics of the latter system. Therefore, if larger PCM product crystals are desired from the PMSMPR unit, modeling and optimization of the system is necessary as highlighted earlier.

An important variable which affects the product crystal quality from the PMSMPR is the seeding protocol employed. In a recent review paper, O'Sullivan et al. [33] highlighted some of the key seeding strategies used in industry to achieve desired product crystal attributes in batch crystallizers, which may also be applied to periodic flow crystallization. The authors highlighted that seeding with crystals of the correct size, mass and form at the right point in a process can lead to more consistent and repeatable crystallizations. Selecting the appropriate seeding conditions (for example, seeding temperature), at the appropriate supersaturation level can lead to improved crystallization outcomes. Here, information on the metastable zone width (MSZW) of the crystallizing system is necessary to determine whether to seed close to the solubility curve or the metastable curve. Another important consideration is the appropriate seed loading and seed

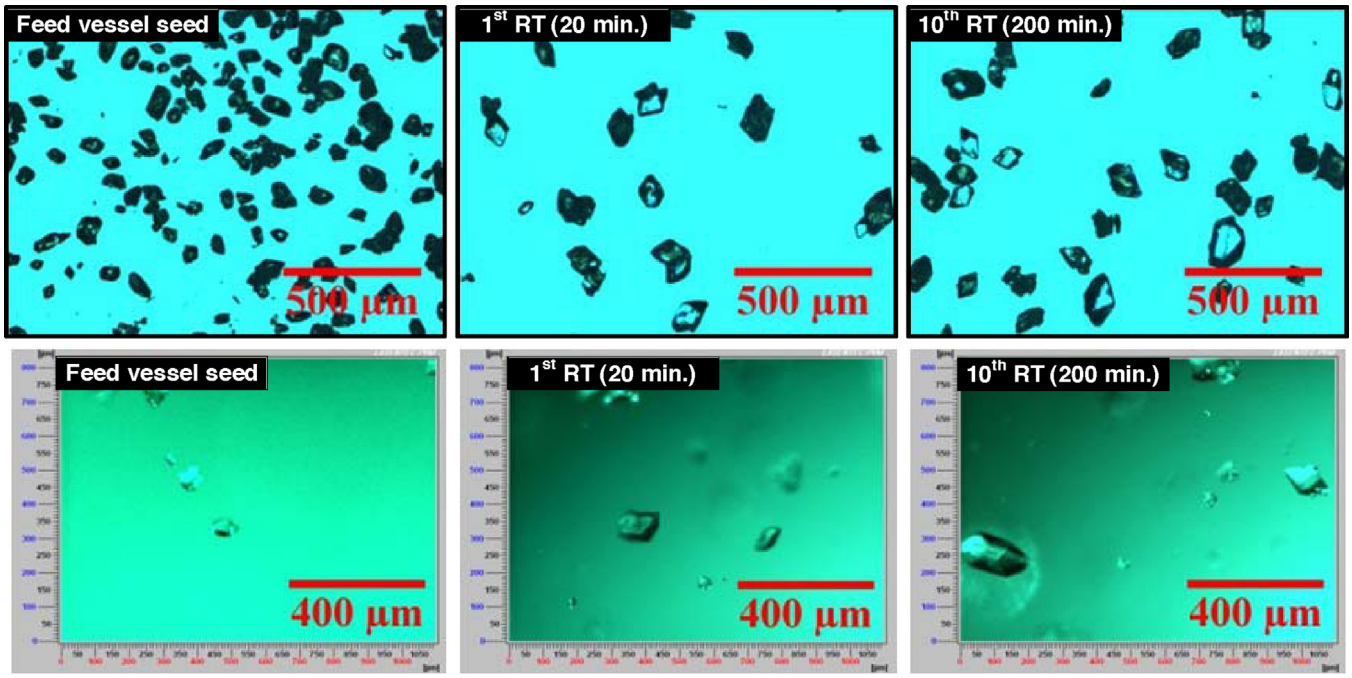

Fig. 12. Microscope (top row) and PVM images (bottom row) of seeds crystals from feed stream, and crystals from the 1st RT (20 min) and 10th RT (200 min) of the single-stage PMSMPR operated with non-concentrated recycle stream (M-P5).

size for a process, which depends on the desired product crystal size, distribution and polymorphic form. Typically, if large crystals are desired, less seed material of larger size is added to encourage growth. On the other hand, if small crystals are desired then a large seed loading of small sized particles are used. In the PMSMPR experiments discussed earlier and preliminary experiments not reported here, both of these seeding strategies were utilized to determine the effect on the crystallization outcome for the PCM-IPA system. The best results, in terms of crystal growth were observed using a seed loading of 2.5% and either 75–125 μm recrystallized seed fraction or 100–125 μm raw material seed fraction. However, only marginal growth was observed in the majority of experiments conducted.

3.3.4. Comparison of PVM and off-line microscope images

PVM images were captured in real-time and off-line microscope images taken of the dried product crystals after each RT in each of the PMSMPR experiments. Fig. 9 shows the off-line microscope images and real-time PVM images for M-P1 (single-stage PMSMPR without recycle) of the seed and product crystals from the 1st and 10th RT respectively.

The images for the 1st and 10th RT show evidence of crystal growth relative to the seed crystals although there are also many fine crystals present, indicative of secondary nucleation, which contributes to reducing the overall SWMCL of the product. The images also show a small number of agglomerates and twinned crystals. Significantly more agglomerates are observed in the microscope images compared to the PVM images. This is not entirely surprising since microscope images were obtained after filtration and drying of product crystals. On filtration, crystals have a tendency to stick together and agglomerates may form as a result of crystals cementing together when mother liquor associated with the wet filter cake becomes supersaturated from solvent evaporation. Furthermore, the outlet slurry is supersaturated when exiting the PMSMPR as shown from the operating region in the phase diagram (Fig. 5).

Fig. 10 shows the microscope and PVM images for M-P2a and M-P2b (single-stage PMSMPRs operated with non-concentrated recycle stream).

Compared to M-P1 seed which shows predominantly regular shaped and sized rhombic crystals, the M-P2a and M-P2b seed crystals appear irregular in shape and size. As discussed earlier in this paper, seed crystals used for M-P2a and M-P2b experimental run were prepared from PCM raw material rather than recrystallized material. The product crystals from the 1st and 10th RTs indicate that there is growth relative to the seeds evidenced from a number of large crystals present. However, there are also a number of agglomerates and fine crystals present. The fine particles present in both the 1st and 10th RT products are indicative of some secondary nucleation, which was confirmed by the time diagrams shown earlier (Fig. 3). These observations agree with the findings from the assessment of the FBRM SWMCL (Table 2) and SWCLD (Figs. 6 and 7).

The seed and product crystals from M-P3 and M-P4 experimental runs, that is, single-stage PMSMPR operated with non-concentrated and concentrated recycle stream, respectively, are shown in the Fig. 11. The PMSMPR product crystals show a characteristic rhombic shape, which is similar to the starting seed material used. Once again, there is evidence of agglomeration from the microscope images of both the seeds (sampled from feed stream) and product crystals, which may be due to the sample preparation process. However, this is not the only cause of crystal agglomeration. It appears that PCM has a natural tendency to agglomerate when many fine crystals are produce from secondary nucleation. There is evidence of agglomeration and crystal twinning from the in situ PVM images of the 1st and 10th RT product crystals.

The images of product crystals for M-P4 show more agglomerates and fines present, although there are also a few large crystals present as well. In particular, the PVM images of the 1st and 10th samples show a significant number of fine crystals present relative to large ones. This suggests that the contribution from secondary

nucleation is more significant than from crystal growth, which is attributed to the concentration of the recycle stream. The operating supersaturation level in M-P4 is higher (1.28) than that of M-P3 (1.23), which was operated with a non-concentrated recycle stream. This is an indication that only a small change in supersaturation can significantly affect the crystallization outcome. The large number of fines observed from the microscope and PVM images also support the SMWCL and SWCLD data from FBRM, both of which indicated that the mean size of the product crystals from M-P4 was smaller compared to the initial seed crystals used.

The steady-state product crystals obtained from the two-stage PMSMPR experimental run (M-P5) were of the best quality of all the PMSMPR configurations investigated. Fig. 12 shows the microscope and PVM images for the seed, 1st RT and 10th RT products, respectively. The images show that relative to the seed crystals there is a small, but noticeable amount of crystal growth which was also confirmed from FBRM SWMCL and SWCLD data presented earlier.

The overall results from M-P5 indicate that with a more controlled and stepwise temperature change in the two-stage PMSMPR, better product properties in terms of crystal size and yield are attainable compared to the single-stage PMSMPR operated with and without recycle stream.

4. Conclusions

Periodic flow crystallization in a novel PMSMPR was demonstrated as a feasible method of producing crystalline material, without encountering operating problems such as fouling, encrustation and blockage of transfer lines. Periodic flow crystallization is a relatively new method whereby controlled disruptions are applied to the crystallizer primarily to increase the mean residence time of the unit and control crystal product attributes such as size and distribution. For the PMSMPR, conventional MSMPR operation is alternated with batch operation to increase mean residence time. This operation illustrates a new paradigm of continuous operation whereby the process is in controlled state of operation (or periodic steady-state) rather than steady-state. The application of an integrated array of PAT tools and in-house developed information system software CryPRINS to the monitoring and characterization of the PMSMPR was also demonstrated.

The indicative CSDs for single-stage PMSMPR (operated with and without recycle stream) and a two-stage PMSMPR (operated without a recycle stream) were determined from FBRM SWCLD data. The indicative mean crystal sizes were determined from FBRM SWMCL data. Steady-state operation was characterized using Raman, ATR-UV/vis, FBRM and PVM. The results indicate that the configuration of the PMSMPR (single- or two-stage), seeding strategy and the use of recycle stream (concentrated or non-concentrated) can affect the crystallization outcome in terms of yield and mean crystal size attainable. The time taken to reach steady-state in the PMSMPR is more or less similar for all experiments except M-P2b, which was conducted using non-concentrated recycle and raw material seed, which was variable in size and shape. This result suggests that the seed properties can influence the time to achieving steady-state. With respect to configuration, the highest yield and mean product crystal size was obtained from the two-stage PMSMPR operated without a recycle stream. Furthermore, the crystal properties in terms of size and shape were noticeably better from the two-stage PMSMPR as observed from PVM and off-line microscope images of product crystals when compared to the product crystal from single-stage PMSMPR experiments. Of the single-stage PMSMPR configurations investigated, the largest mean crystal size was obtained from the system without recycle stream (M-P1). In comparison, the configuration with non-concentrated recycle stream (M-P3) gave a marginally smaller mean size. Although the single-stage PMSMPR with concentrated recycle stream (M-P4) gave a higher yield, the mean crystal size of the periodic steady-state product was markedly smaller. This is a further indication that concentrating the recycle stream improves process yield, but leads to smaller crystals due to increased secondary nucleation in the system. In all of the other PMSMPR experiments reported there was evidence of growth relative to the seed crystals used. However, the extent of crystal growth observed in all experiments, except M-P2b was marginal due to the strong influence of secondary nucleation on the crystallization mechanism of PCM. The result from M-P2b showed a significant shift of the periodic steady-state product SWCLD to larger sizes relative to the seed crystals used. This result suggests that the seed properties can also influence the steady-state product CSD. Agglomeration and growth were both evident in the periodic steady-state product as confirmed by PVM and microscope images. A batch crystallization experiment was also conducted under similar conditions to that of the PMSMPR experiments for evaluation and comparison. As expected, the yield of the batch crystallization process was higher than in all of the PMSMPR experiments. However, the product crystals were significantly smaller, indicative of a broad CSD as confirmed by FBRM, PVM and off-line microscope image analysis. This was due to a significant amount of secondary nucleation in the batch system compared to the PMSMPR systems. Information from the batch crystallization experiment gave further evidence that secondary nucleation is the dominant crystallization mechanism of PCM even at low supersaturation levels. It was inferred from the observations in the batch crystallization study, that PMSMPR is effective at controlling the extent of secondary nucleation leading to crystals of larger size compared to the seed materials used, albeit marginal in most cases. Robust monitoring and temperature control using integrated PAT array and CryPRINS information systems software [30] was also demonstrated for the periodic flow crystallization in the PMSMPR. The results indicate that the combined used of PAT and information systems can indicate when the periodic flow process reaches steady-state and also provides a better understanding of the parameters and operating procedures that influence the periodic steady-state operation. While the periodic operation was demonstrated here for seeded cooling crystallization, a similar approach can be applied for anti-solvent or combined cooling and anti-solvent systems [31]. The periods of alternating continuous and batch operation can be tailored to accommodate crystallization systems belonging to different classes based on their growth and nucleation kinetics [32].

Acknowledgments

The authors would like to thank the EPSRC (EP/I033459/1) and the Centre for Continuous Innovation in Continuous Manufacturing and Crystallization (CMAC) for the financial support of this work and the European Research Council under the European Union's Seventh Framework Programme (FP7/2007-2013)/ERC grant agreement no. [280106-CrySys] (for equipment and financial support).

References

[1] L.X. Yu, R.A. Lionberger, A.S. Raw, R. D'Costa, H. Wu, A.S. Hussain, Adv. Drug Deliv. Rev. 56 (2004) 349–369.
[2] X.Y. Woo, Z.K. Nagy, R.B.H. Tan, R.D. Braatz, Cryst. Growth Des. 9 (2009) 182–191.
[3] M. Barrett, M. McNamara, H. Hao, P. Barrett, B. Glennon, Chem. Eng. Res. Des. 88 (2010) 1108–1119.
[4] N. Gherras, E. Serris, G. Fevotte, Int. J. Pharm. 439 (2012) 109–119.
[5] Y. Hu, J.K. Liang, A.S. Myerson, L.S. Taylor, Ind. Eng. Chem. Res. 44 (2005) 1233–1240.

[6] A.N. Saleemi, G. Steele, N.I. Pedge, A. Freeman, Z.K. Nagy, Int. J. Pharm. 430 (2012) 56–64.
[7] Z.K. Nagy, M. Fujiwara, R.D. Braatz, J. Process Control 18 (2008) 856–864.
[8] E. Simone, A.N. Saleemi, Z.K. Nagy, Chem. Eng. Res. Des. 92 (2014) 594–611.
[9] H. Wu, M. White, R. Berendt, R.D. Foringer, M. Khan, Ind. Eng. Chem. Res. 53 (2014) 1688–1701.
[10] L.L. Simon, T. Merz, S. Dubuis, A. Lieb, K. Hungerbuhler, Chem. Eng. Res. Des. 90 (2012) 1847–1855.
[11] Z.K. Nagy, G. Fevotte, H. Kramer, L.L. Simon, Chem. Eng. Res. Des. 91 (2013) 1903–1922.
[12] E. Kougoulos, A.G. Jones, K.H. Jennings, M.W. Wood-Kaczmar, J. Cryst. Growth 273 (2005) 529–534.
[13] E. Kougoulos, A.G. Jones, M.W. Wood-Kaczmar, J. Cryst. Growth 273 (2005) 520–528.
[14] A.J. Alvarez, A.S. Myerson, Cryst. Growth Des. 10 (2010) 2219–2228.
[15] J.L. Quon, H. Zhang, A.J. Alvarez, J.M.B. Evans, A.S. Myerson, B.L. Trout, Cryst. Growth Des. 12 (2012) 3036–3044.
[16] H. Zhang, J.L. Quon, A.J. Alvarez, J.M.B. Evans, A.S. Myerson, B.L. Trout, Org. Process Res. Dev. 16 (2012) 915–924.
[17] A.J. Alvarez, A. Singh, A.S. Myerson, Cryst. Growth Des. 11 (2011) 4392–4400.
[18] S. Ferguson, G. Morris, H. Hao, M. Barrett, B. Glennon, Chem. Eng. Sci. 104 (2013) 44–54.
[19] G. Hou, G. Power, M. Barrett, B. Glennon, G. Morris, Y. Zhao, Cryst. Growth Des. (2014) 1–34.
[20] L.L. Simon, A.S. Myerson, Associazione Italiana Di Ingegneria Chimica (AIDIC), (2011) , pp. 3–6.
[21] R. Whelan, M. Barrett, H. Hao, B. Glennon, 11th International Conference on Chemical and Process Engineering, Milan, 2013, pp. 1–4.
[22] S. Ferguson, G. Morris, H. Hao, M. Barrett, B. Glennon, Chem. Eng. Sci. 77 (2012) 105–111.
[23] A. Gerstlauer, S. Motz, Chem. Eng. Sci. 57 (2002) 4311–4327.
[24] A.D. Randolph, M.A. Larson, AIChE J. 8 (1962) 639–645.
[25] A.D. Randolph, M.A. Larson, Theory of Particulate Processes, Academic Press, New York, 1971.
[26] J. Nývlt, O. Söhnel, M. Matachová, M. Broul, AIChE J. 32 (1986) 1231.
[27] M.R.H.A. Bakar, Process Analytical Technology Based Approaches for the Monitoring and Control of Size and Polymorphic Form in Pharmaceutical Crystallisation Processes, Loughborough University, 2010.
[28] J. Garside, M.B. Shah, Ind. Eng. Chem. Process Des. Dev. 19 (1980) 509–514.
[29] A.N. Saleemi, C.D. Rielly, Z.K. Nagy, Cryst. Growth Des. 12 (2012) 1792–1807.
[30] A.D. McNaught, A. Wilkinson, IUPAC Compendium of Chemical Terminology, in: A.D. McNaught, A. Wilkinson (Eds.), 2nd ed., 2006.
[31] E. Aamir, Z.K. Nagy, C.D. Rielly, Cryst. Growth Des. 10 (2010) 4728–4740.
[32] M. Fujiwara, P.S. Chow, R.D. Braatz, Cryst. Growth Des. 2 (2002) 363–370.
[33] B. O'Sullivan, B. Smith, G. Baramidze, Mettler Toledo White Paper: Recent Advances for Seeding a Crystallization Process A Review of Modern Techniques Crystallization Development, (2013) , pp. 3–12.
[34] N. Doki, N. Kubota, A. Sato, M. Yokota, Chem. Eng. J. 81 (2001) 313–316.